

Budapest Neutron Centre Centre for Energy Research

Cross-section measurements in
slow-neutron beams

László Szentmiklósi, Tamás Belgya, Zsolt Révay

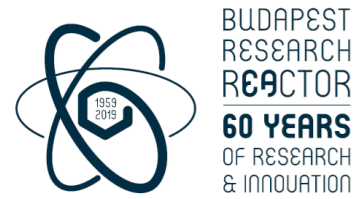
ARIEL Training School, Budapest, Hungary

Budapest Neutron Centre, Budapest, Hungary

szentm@bnc.hu

Nuclear Analysis and Radiography Department
Centre for Energy Research, Budapest, Hungary

szentmiklosi.laszlo@ek.hun-ren.hu



Budapest Neutron Centre Centre for Energy Research

Nuclear reactions,
quantities related to the
neutron capture





The neutron is a neutral particle with mass of $1.67492716 \times 10^{-27}$ kg, 1.00866491560(55) dalton, 939.565360(81) MeV

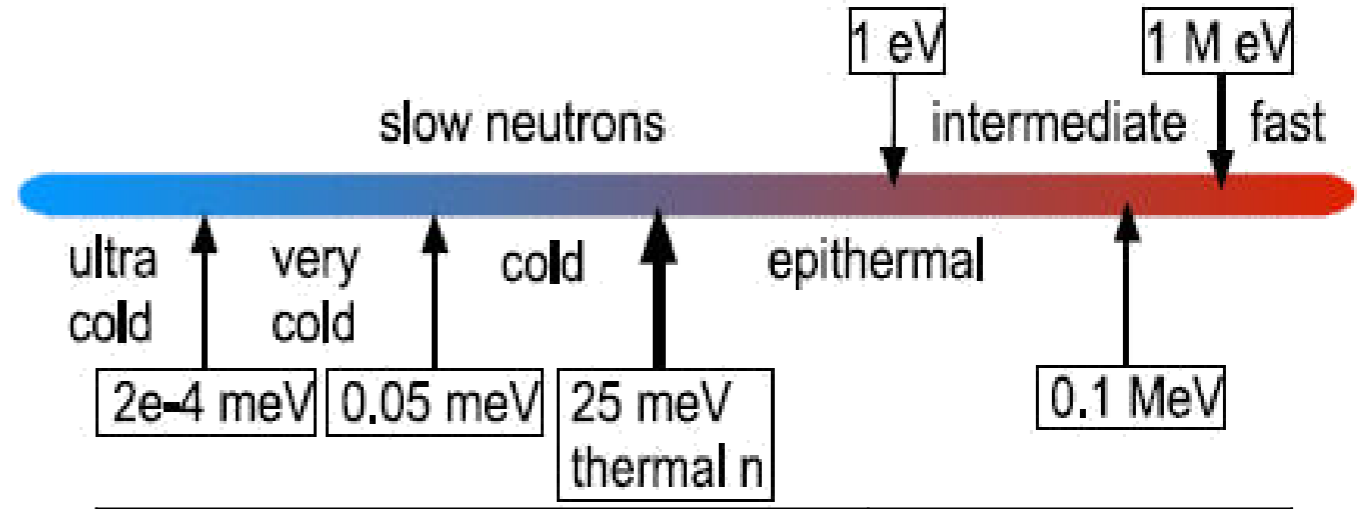
The free neutron is unstable, **decays** with a half-life of $T_{1/2} = 885.7 \pm 0.8$ s to a proton, an electron and an anti-electronneutrino.

Free neutrons can be produced only by nuclear reactions.

The **neutrons are classified** according to the kinetic energy

Moderation: the neutron comes to a thermal equilibrium with the ambient media as it passes through a material. Using a cold material, the velocity of neutrons can be decreased.

*1 eV = $1.602176462(63) \times 10^{-19}$ J



		Energy
Slow neutrons	Ultracold	$< 10^{-5}$ eV
	Cold	10^{-5} -- 0,025 eV
	Thermal	$\sim 0,025$ eV
	Epithermal	0,025 -- 1 eV
	Resonance	1 -- 1000 eV
Intermediate-energy neutrons		1 -- 1000 keV
Fast neutrons		0.1 -- 10 MeV
High-energy neutrons		> 10 MeV

$$A(b,c)D = A + b \rightarrow c + D (+ Q)$$

A – target nucleus

D – final nucleus

b - projectile

c – emitted particle

Q – reaction energy (+ exotherm, - endotherm)

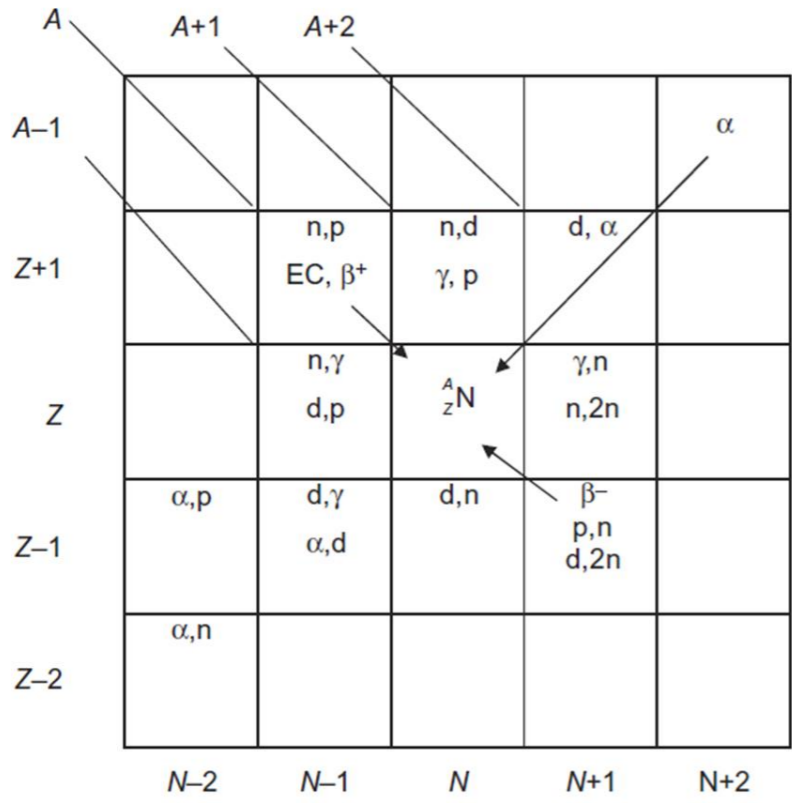


Figure 6.10 Summary of different options to produce a nuclide with Z atomic number and A mass number. It includes the formation of the nuclide by radioactive decays as well.

	Ga64 2.627 m 0+	Ga65 15.2 m 3/2-	Ga66 9.49 h 0+	Ga67 3.2612 d 3/2-	Ga68 67.629 m 1+	Ga69 3/2-
	EC	EC	EC	EC	EC	60.108
	Zn63 38.47 m 3/2-	Zn64 0+	Zn65 244.26 d 5/2-	Zn66 0+	Zn67 5/2-	Zn68 0+
	EC	48.6	EC	27.9	4.1	18.8
Cu61 3.333 h 3/2-	Cu62 9.74 m 1+	Cu63 3/2-	Cu64 12.700 h 1+	Cu65 3/2-	Cu66 5.088 m 1+	Cu67 61.83 h 3/2-
EC	EC	69.17	EC,β ⁻	30.83	β ⁻	β ⁻
Ni60 0+	Ni61 3/2-	Ni62 0+	Ni63 100.1 y 1/2-	Ni64 0+	Ni65 2.5172 h 5/2-	Ni66 54.6 h 0+
26.225	1.140	3.634	β ⁻	0.926	β ⁻	β ⁻
Co59 7/2-	Co60 5.2714 y 5+	Co61 1.650 h 7/2-	Co62 1.50 m 2+	Co63 27.4 s (7/2)-	Co64 0.30 s 1+	Co65 1.20 s (7/2)-
100	*	β ⁻	β ⁻	β ⁻	β ⁻	β ⁻

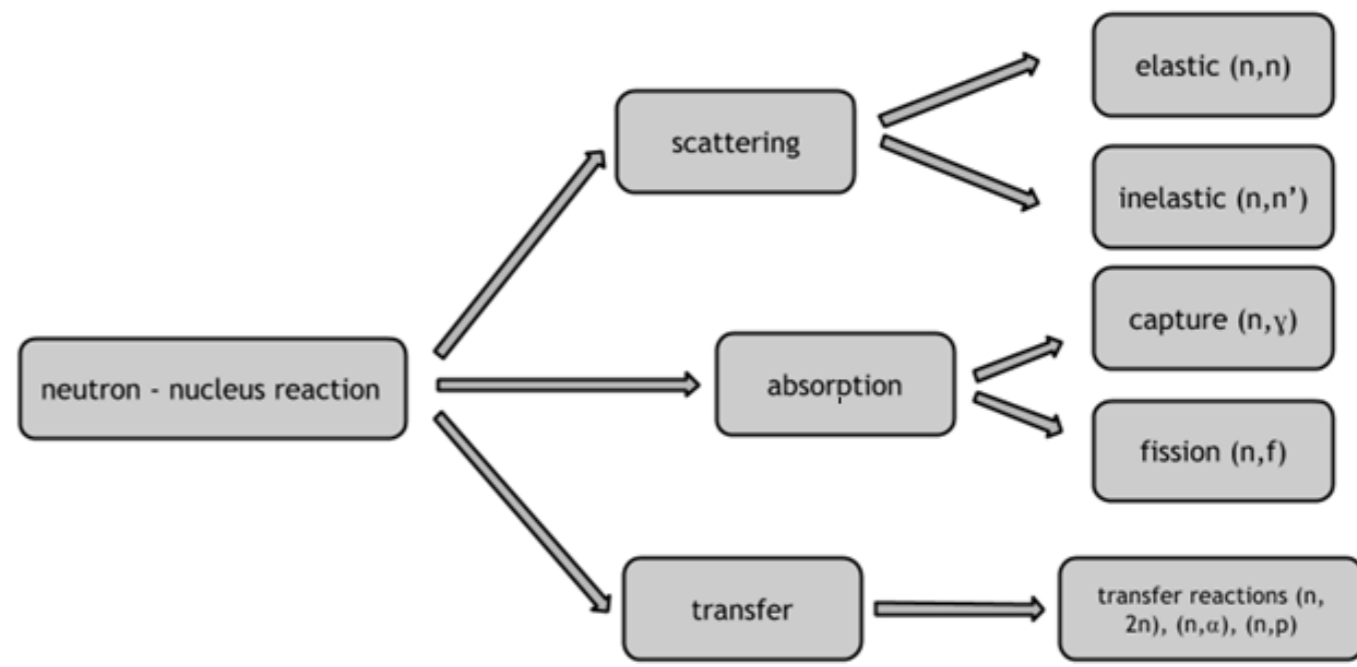
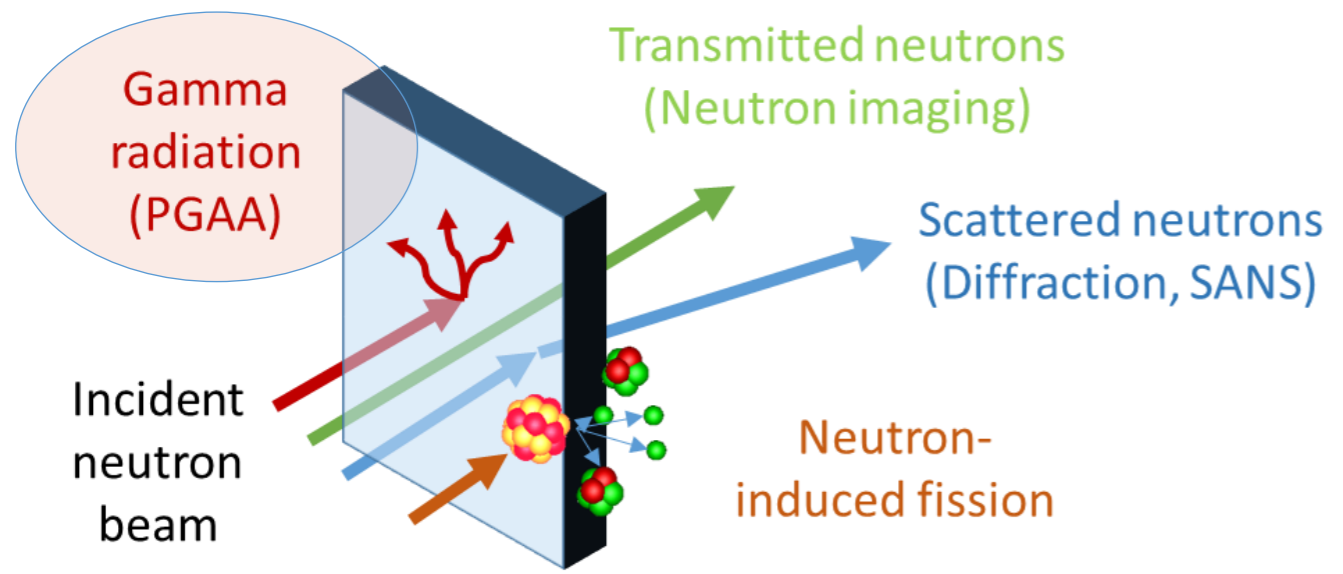


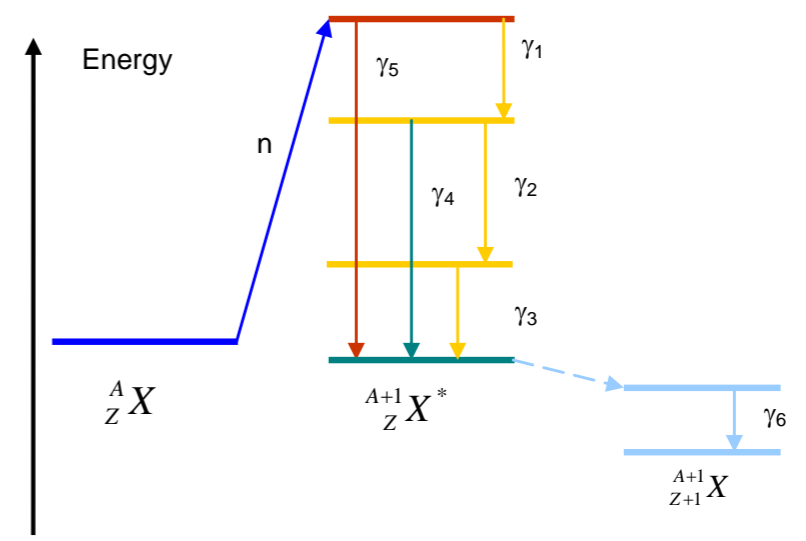
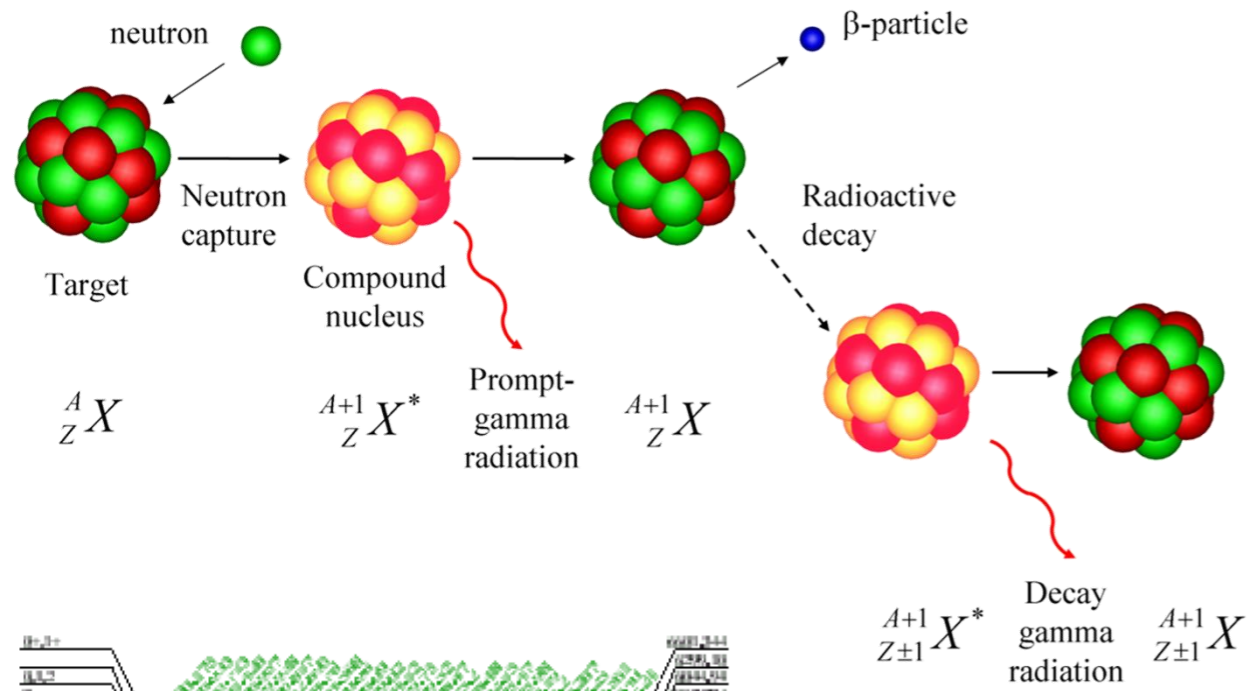
IAEA Isotope Browser App



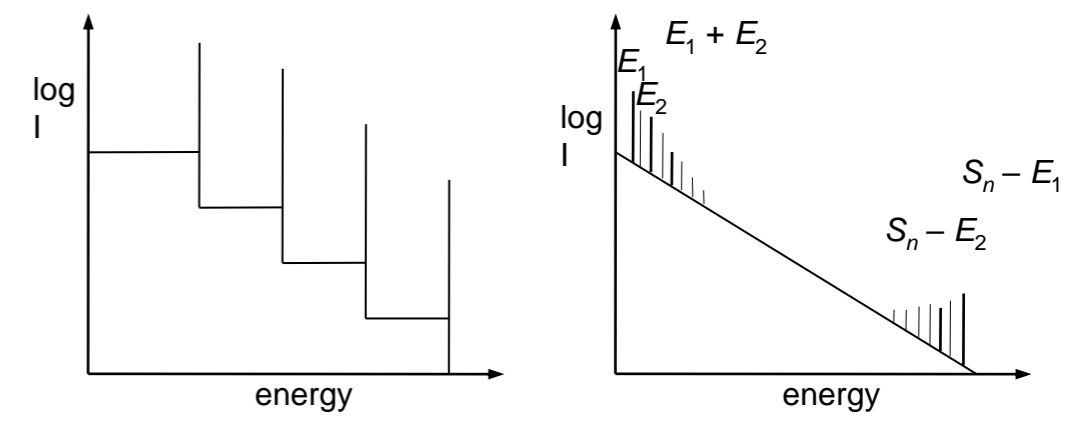
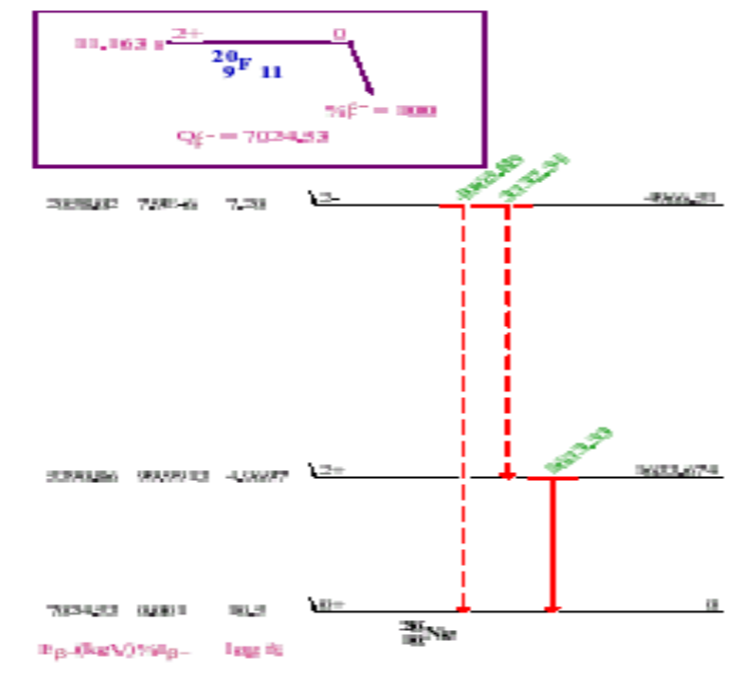
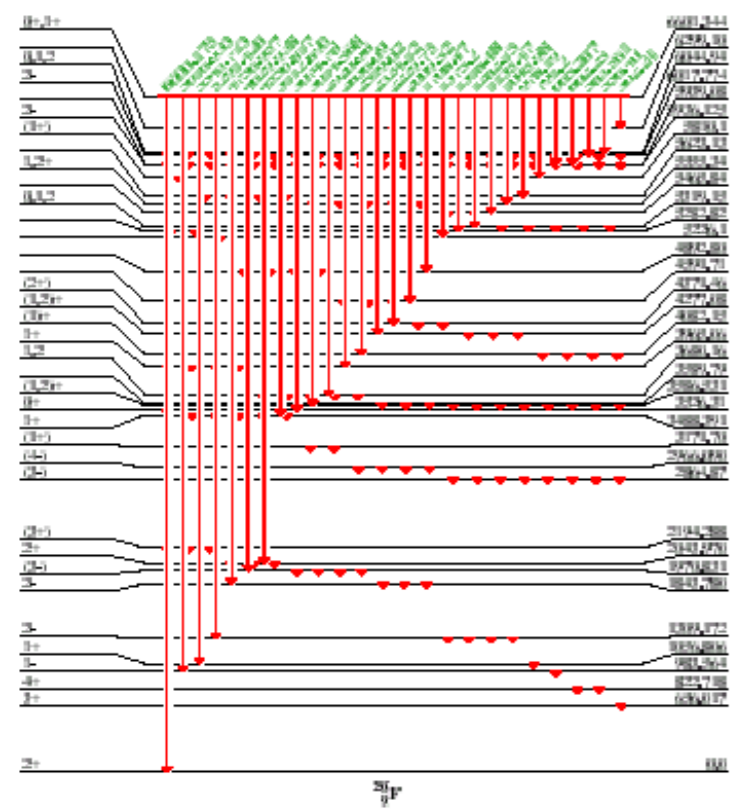
Neutrons interact with the condensed matter:

- Induce nuclear reactions (capture, fission)
- Scattering (elastic, inelastic)
- Reflection
- Unaffected neutrons pass through the sample



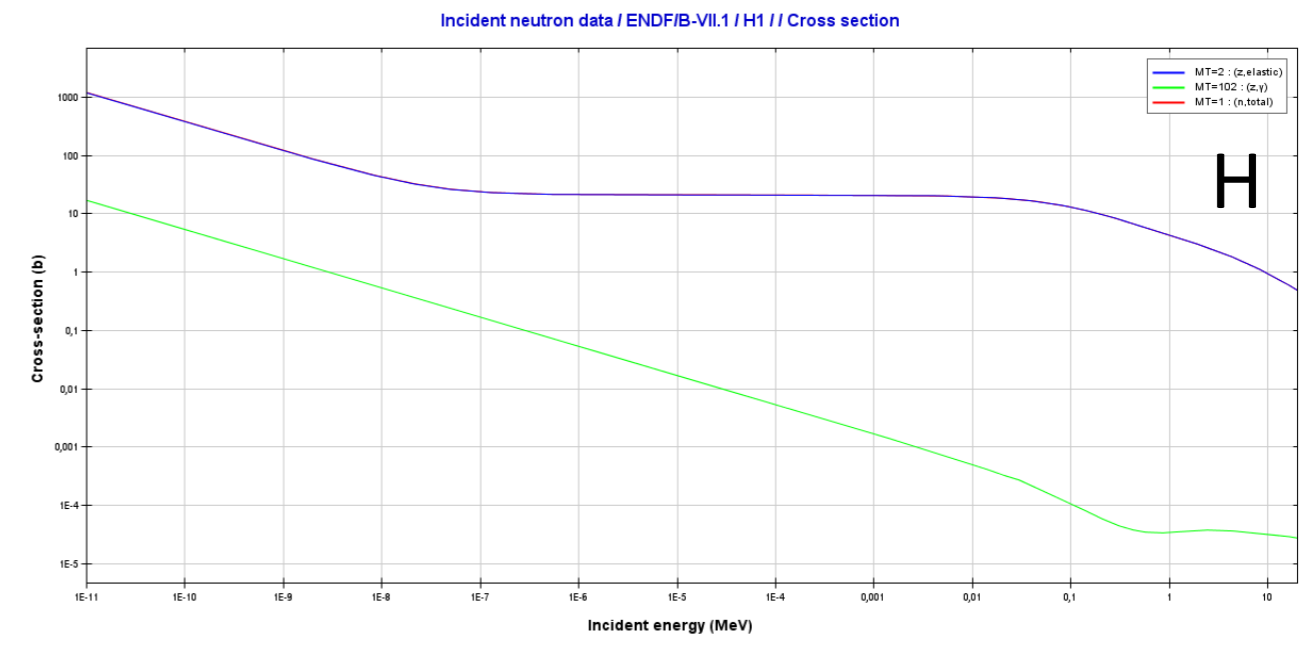
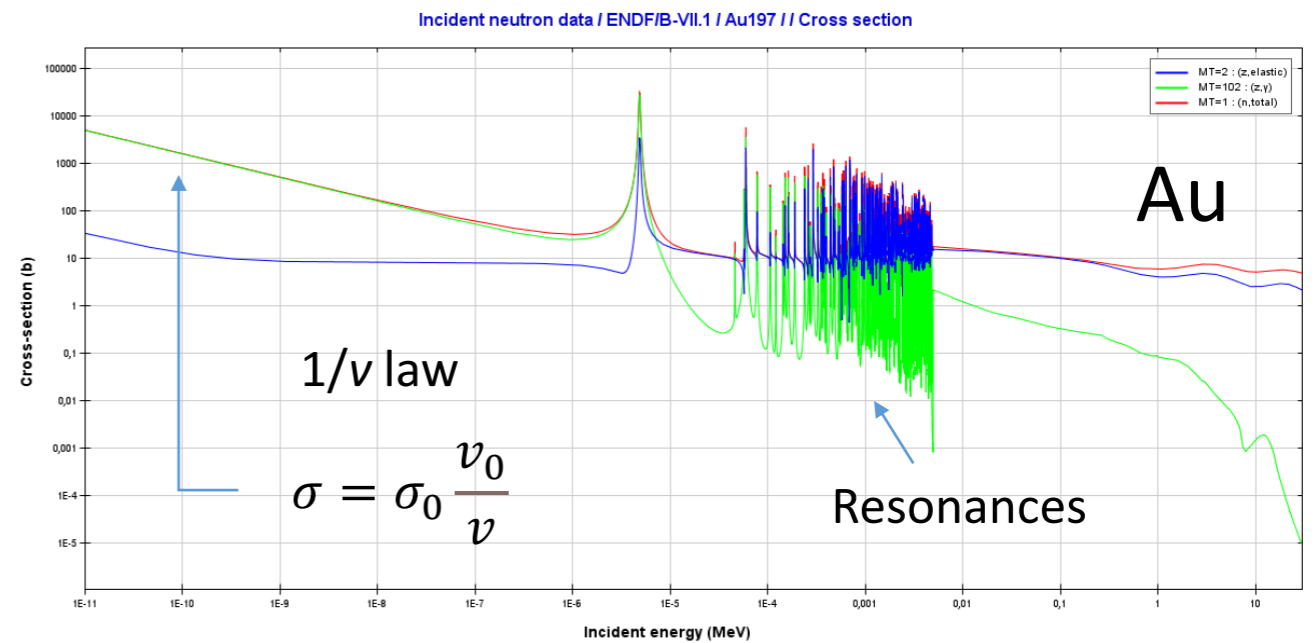


Capture gamma spectrum:





- The neutron capture cross section of an isotope of a chemical element is the apparent cross-sectional area that an atom of that isotope presents to absorption and is a measure of the probability of neutron capture.
- It is usually measured in barns, i.e. 10^{-24} cm² or 10^{-28} m²
- Capture cross section is highly dependent on neutron energy. This is called excitation function or energy-differential cross-section
- The cross-section of neutrons with 2200 m/s velocity is called thermal neutron capture cross section
- At low kinetic energies, the likelihood of absorption is proportional to the time the neutron is in the vicinity of the nucleus. The time spent in the vicinity of the nucleus is inversely proportional to the relative velocity between the neutron and nucleus. This is the 1/v law.
- One expect the highest reaction rate per atom for cold neutrons
- Neutrons should be moderated or cooled to maximize the capture reaction rate





- The cross-section of monochromatic neutrons with velocities of 2200 m/s characteristic of the thermal beam is the same for most nuclides as for neutrons following Maxwell's distribution with an energy of 0.025 eV and a temperature of 293 K, therefore this value is called thermal and is denoted by σ_0 .
- However, the absorbed neutron may also produce a gamma-continuum, so the capture cross-section alone is not suitable for characterizing detectability of a gamma peak.
- The probability of emitting a prompt-gamma photon of a certain energy is characterized by the partial gamma-ray production cross-section (σ_γ). This is the spectroscopically characteristic parameter that is also used in PGAA for quantitative elemental composition analysis. The relationship between the two quantities is:

$$\sigma_\gamma = \theta P_\gamma \sigma_0$$

where θ is the isotopic abundance and P_γ is the emission probability.



If we sum up all the probabilities of emission, we get the average number of transitions in which the excited nucleus reaches the ground state

Element	$\sum_i P_{g,i}$
H	1
Be	1.57
C	1.50
N	2.14
F	3.78
Al	2.98
Cl	2.72
K	3.32
Ti	2.78
Mn	3.52
Fe	1.78
Cd	2.1
Au	2.47
Pb	1.02
Bi	3.49

It follows from the law of energy conservation that the nuclide always radiates the entire excitation energy as it steps through the cascade. Thus, if we sum the energies of all relevant gamma lines weighted by the emission probabilities, we get the binding energy of the neutron, i.e.

$$S_n = \sum_i E_{\gamma,i} P_{\gamma,i} \quad 1 = \sum_i \frac{E_{\gamma,i}}{S_n} \frac{\sigma_{\gamma,i}}{\sigma_0}$$

If values greater than a certain partial cross-section threshold, e.g. 10 %, are included in the summation, the number obtained expresses how strong the gamma lines are.

A few very intense transitions or many smaller?

60	Nd	7566	22.8	9.49
62	Sm	7961	11.4	7.15
63	Eu	6314	0.74	0.45
64	Gd	8048	8.18	0.36
65	Tb	6375	0.14	0
66	Dy	6473	13.5	0.44
67	Ho	6244	3.03	0.77
68	Er	7736	10.4	4.31

Z	El.	$\langle S_n \rangle$ (keV)	Q(1%)	Q(10%)
1	H	2225	100	100
3	Li	2368	100	72.7
4	Be	6812	100	100
5	B	478 ^a	100	100
6	C	4960	100	100
7	N	10833	100	84.2
8	O	4147	100	100
9	F	6601	80.5	8.4
10	Ne	6759	93.2	69.3
11	Na	6959	87.1	53.2
12	Mg	8398	94.0	56.3
13	Al	7725	70.9	21.6
14	Si	8496	99.4	83.4
15	P	7936	79.6	40.7
16	S	8625	96.9	77.8
17	Cl	8572	75.0	29.1
18	Ar	6169	92.2	65.2
19	K	7791	66.1	4.63
20	Ca	8356	83.7	61.3
21	Sc	8761	38.5	2.23
22	Ti	8273	100	82.4
23	V	7423	86.8	28.9
24	Cr	9237	92.0	41.9
25	Mn	7270	61.9	11.9
26	Fe	7778	84.7	48.5
27	Co	7492	59.2	2.42
28	Ni	8544	80.9	60.6
29	Cu	7766	73.9	38.8



- Multiple gamma photons (gamma cascades) with energies of 30 keV - 11 MeV.
- For N levels, the number of transitions is theoretically possible $N(N-1)/2$, but many of these transitions are prohibited by selection rules
- Even existing transitions may not be detectable with sufficient accuracy
- In the transition between E2 and E1, the energy of the emitted photon is

$$E_2 - E_1 = E_\gamma^{21} + \Delta E$$

where the recoil energy

$$\Delta E = \frac{E_\gamma^2}{2mc^2}$$

- So, the gamma energy we observe slightly differs from the energy of the related nuclear level



- The sum of the signed intensities of photons populating and depopulating an intermediate level is zero. (Particle conservation)
- The sum of the relative intensity-weighted -energies shall be equal to the binding energy of the neutron, this is the so-called "Q-test":

$$\frac{\sum E_{\gamma} \cdot I_{\gamma}}{\sum_{GS} I_{\gamma}} = E_Q$$

where the intensities of gammas arriving at the ground state are summed up in the denominator.

- The prerequisite for the correct value for the level scheme is
 - unbiased energy determination and
 - accurate intensity measurement



- For slow neutron beams only

- Reaction rate in monochromatic beam

$$R = n\sigma\Phi$$

- Experimental observable: peak count rate at E_γ

$$\frac{A}{t} = r_\gamma = n\sigma_\gamma\Phi\varepsilon(E_\gamma)$$

- Theoretical count rate of a γ -peak

$$r_\gamma = \int_V \int_0^\infty \frac{\rho(\mathbf{x})}{M} N_A \sigma_\gamma(E_n) \Phi'(E_n, \mathbf{x}) \varepsilon'(E_\gamma, \mathbf{x}) dE_n d\mathbf{x}$$

including sample and beam inhomogeneity, neutron beam's energy spectrum, spatial dependence of the efficiency via a position vector \mathbf{x}

- This is far too complicated in practice, so simplifications are made...

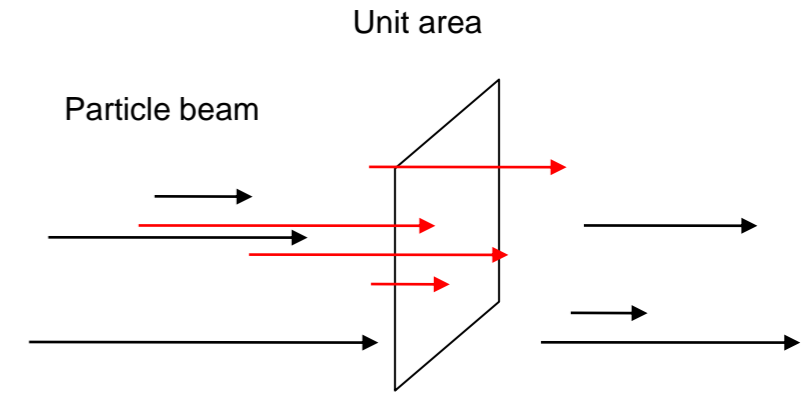
As far as the 1/v law holds, and the sample and the beam are homogeneous, we introduce the concept of thermal-equivalent flux

- σ_0 is the cross-section at 2200 m/s

$$R^0 = n\sigma_0\Phi_0 \quad r_\gamma^0 = \frac{m}{M} N_A \sigma_{\gamma 0} \Phi_0 \varepsilon(E_\gamma)$$



$$\Phi_0 = \int_0^{\infty} \frac{v_0}{v} \Phi(v) dv = \Phi_r \int_0^{\infty} \frac{v_0}{v} \phi(v) dv = \Phi_r \int_0^{\infty} \frac{v_0}{v} \frac{v}{\langle v \rangle} n(v) dv = \frac{v_0}{\langle v \rangle} \Phi_r$$



where Φ_r is the actual flux, i.e. the number of neutrons passing through a unit surface area in a unit time, $\Phi(v)$ is the flux density, $n(v)$ is the neutron density (both density functions are integral per unit of velocity over the entire range), $\langle v \rangle$ is the average velocity derived from the latter distribution.

The "trick" of this transformation is to transfer the $1/v$ dependence of the cross-section to the flux, just by using the thermal cross-section in our subsequent equations

Next, the velocity-dependent flux is converted into the product of the actual flux (Φ_r) and the flux density ($\Phi(v)$). Since integration cannot be done in this way, the flux density is further converted into neutron density: $\Phi(v) = v/\langle v \rangle n(v)$.

Then the velocity v cancels from the equation and the integral of the density function is one. The mean velocity $\langle v \rangle$, in guided and cold beams, is lower than the thermal velocity, so that the reaction rate increases, so that the thermal equivalent flux is typically 2–4 higher than the actual flux

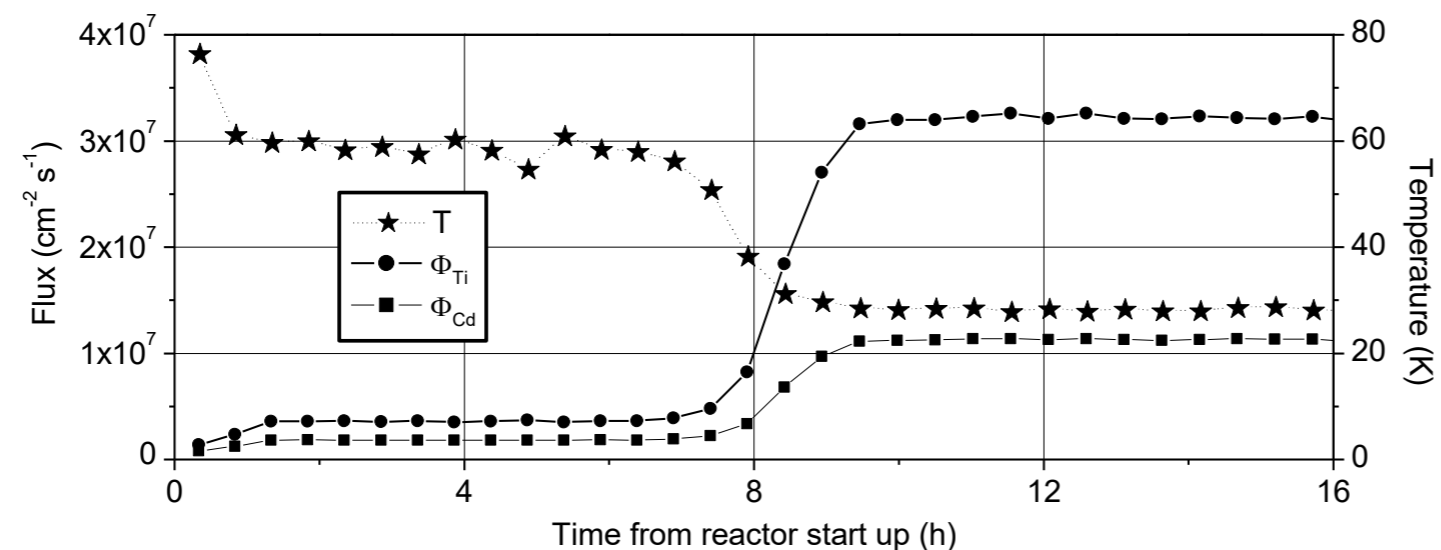
Instead of looking for the real number of impinging neutrons we characterize their effect on the measurable, i.e., the capture rate

- In the other extreme case, the sample has such a large neutron capture cross-section or thickness that it absorbs all neutrons
- In this case, all neutrons that have entered the sample are finally captured and the related gammas are emitted.

$$r_{\gamma}^{\infty} = S\Phi_r P_{\gamma} \varepsilon(E_{\gamma})$$

where S is the beam surface area of the sample (assuming it is less than the beam cross-section), Φ_r is the actual flux, P_{γ} is the emission probability, ε is the peak efficiency of the gamma detector.

- This way the actual flux can be directly determined or, if already known, emission probabilities can be derived.
- The method for determining beam temperature is based on the comparison of actual and thermal equivalent flux



- Thin Ti foil – thermal eq. flux
- Cd plate – real number of impinging neutrons



$$A_\gamma = m \cdot S \cdot t; \quad S = \frac{N_A}{M} \cdot \underbrace{\theta \cdot \sigma_0 \cdot P_\gamma}_{\sigma_\gamma} \cdot \phi \cdot \varepsilon(E_\gamma) \cdot f(E_\gamma)$$

Fit from the (n,g) spectrum

From detector calibration

The use of (n,γ) reaction for elemental composition determination of unknown samples

m : Mass of the element

S : Sensitivity of the analytical peak (cps / mg)

t : measurement time (s)

A_γ : Peak area

N_A : Avogadro-number

M : Molar weight

θ : Isotopic abundance

σ_0 : Neutron capture cross-section

P_γ : Gamma-yield per neutron capture

ϕ : Thermal equivalent neutron flux

$\varepsilon(E_\gamma)$: Detector efficiency

$f(E_\gamma)$: Matrix effect correction (neutron self shielding, gamma self absorption)

Budapest Neutron Centre Centre for Energy Research



Instrumentation



- 10 MW thermal power
- Tank type, Water-cooled, Water-moderated
- 60+ years of operation
- Max. thermal flux in the core: $2 \times 10^{14} \text{ cm}^{-2} \text{ s}^{-1}$



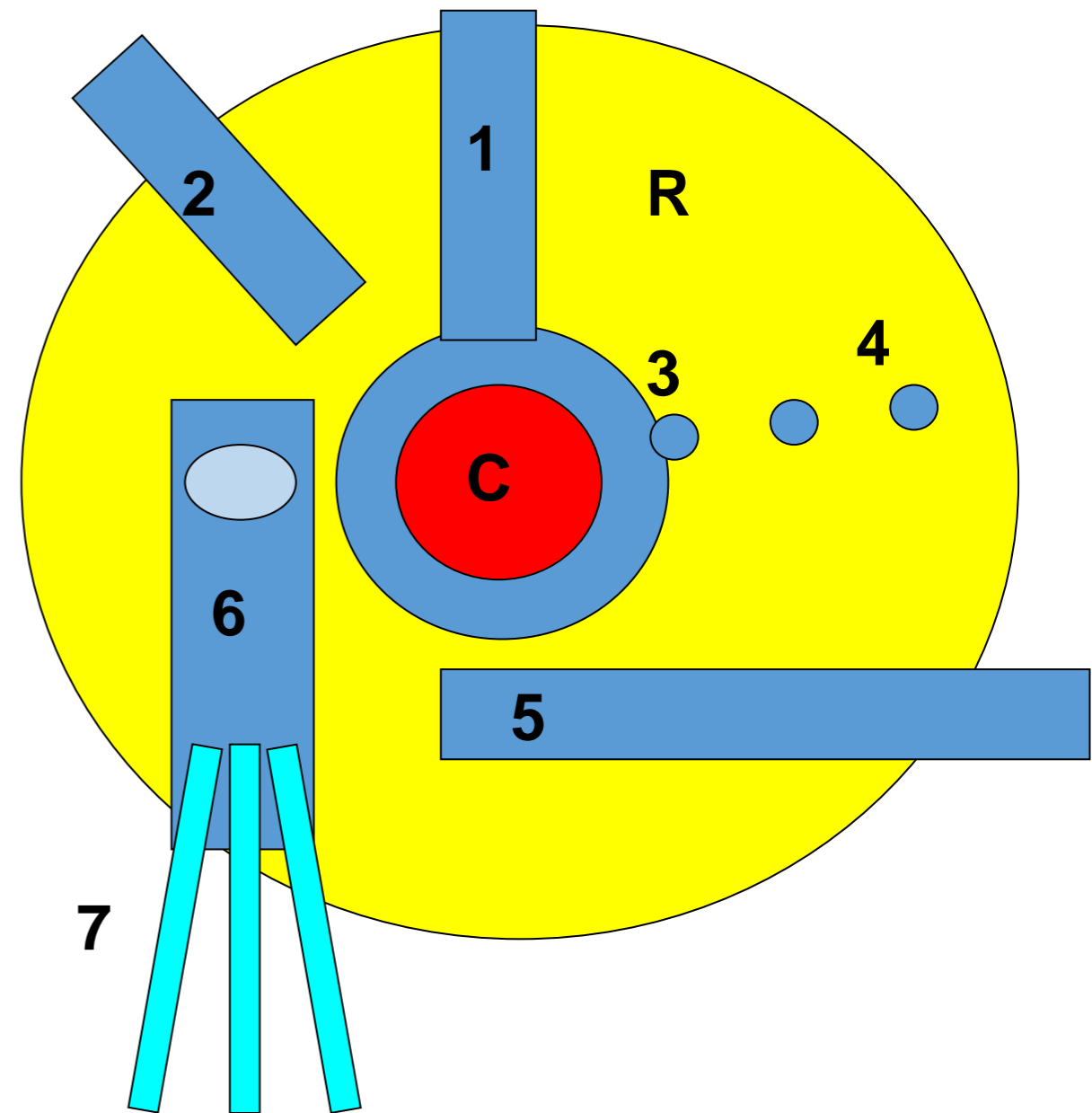
Reactor type:	Tank-type with beryllium reflector, cooled and moderated with light water
Vessel:	Al-alloy (height: 5685 mm; \varnothing 2300 mm)
Core geometry:	Hexagonal (length: 600 mm; \varnothing 1000 mm)
Fuel:	LEU VVR-M2 (19,75 %)
Equilibrium core	190 fuel elements (5x38 age-group FAs)
Control:	18 control rods = 3 safety rods (B_4C); 14 shim rods (B_4C); 1 automatic control rod (SS - Stainless Steel)
Thermal power:	10 MW
Mean power density:	61.2 kW/litre (in the core)
Neutron flux density in the core:	$2,2 \times 10^{14} \text{ n/cm}^2\text{s}$ (thermal in flux traps) $E_n < 0.625 \text{ eV}$ $1 \times 10^{14} \text{ n/cm}^2\text{s}$ (in fast channels) $E_n > 0.5 \text{ MeV}$
Cooling systems:	Two closed loops (primary and secondary loops)
Pr.cooling water:	Q_{nominal} : 1650 m ³ /h; T_{inlet} : 45 °C; T_{outlet} : 50 °C

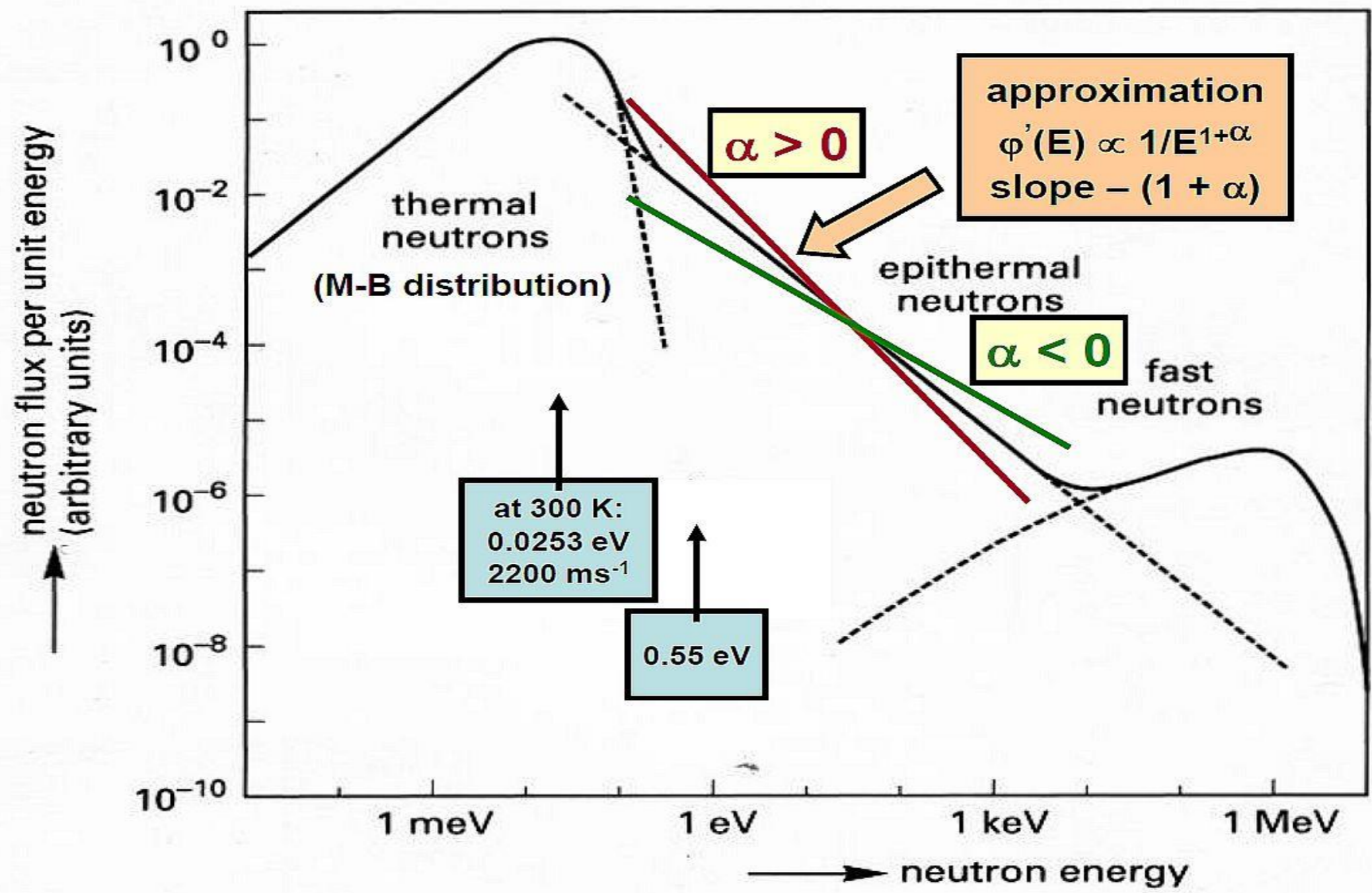




- 1 fast horizontal channel
- 2 thermal horizontal channel
- 3 fast vertical channel
- 4 thermal vertical channel
- 5 tangential channel
- 6 tangential channel with a cold source
- 7 neutron guides

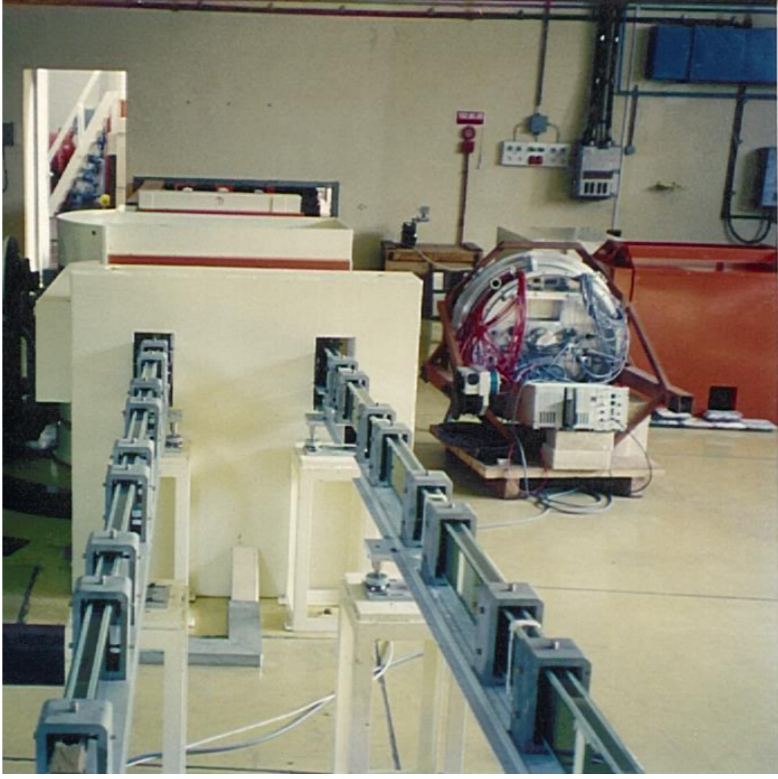
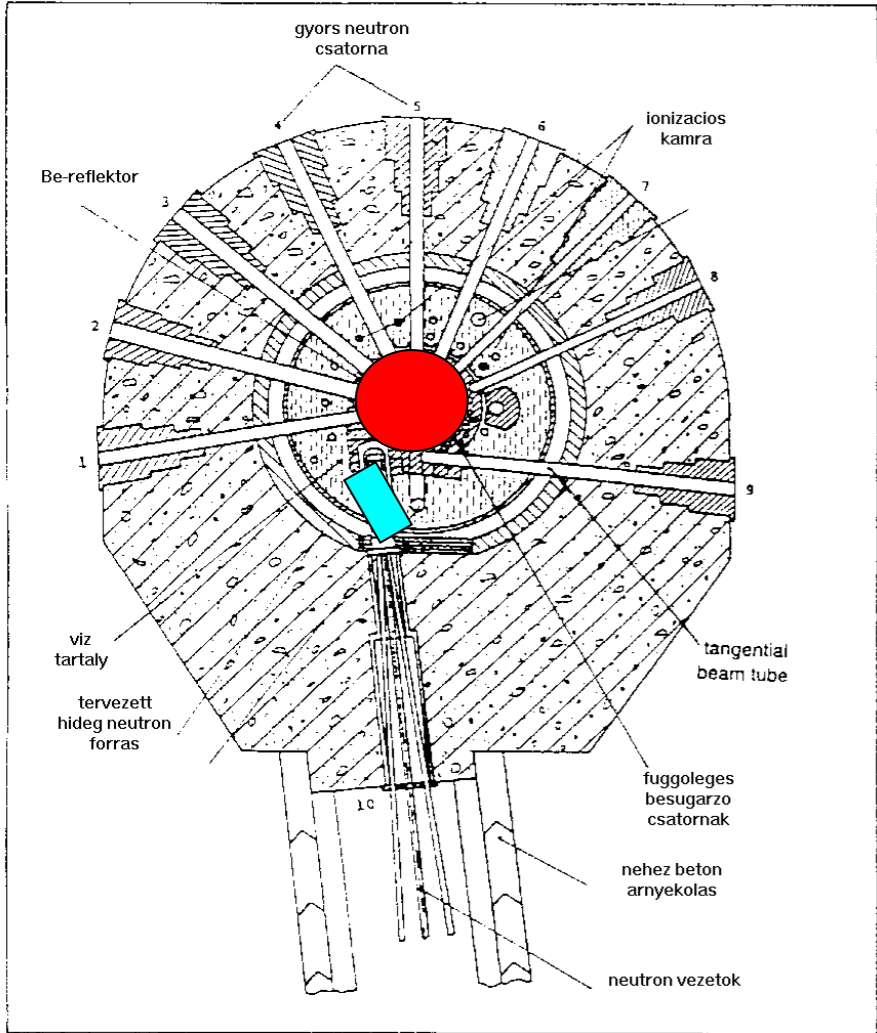
R reflector
C core

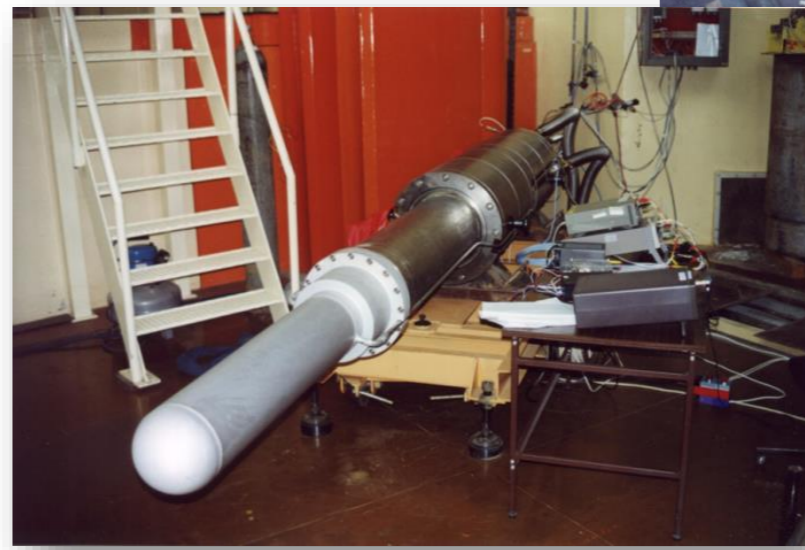
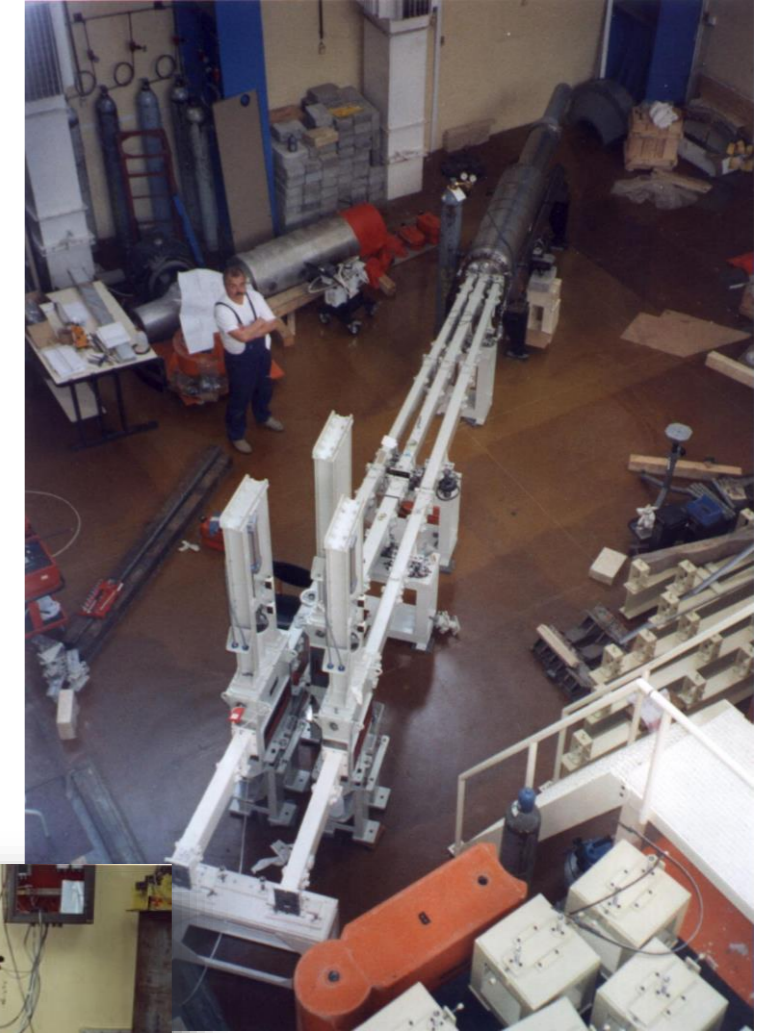
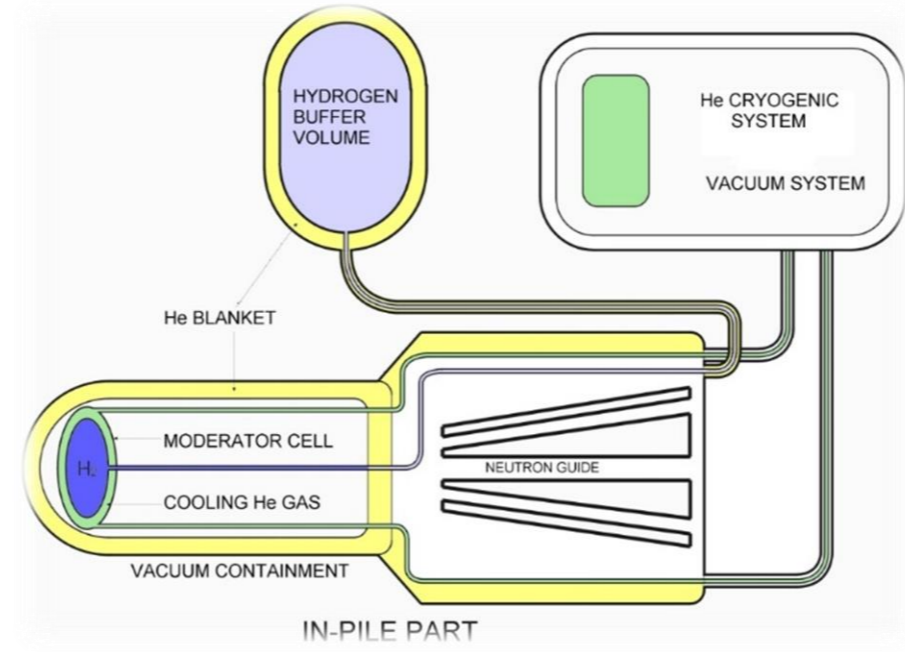
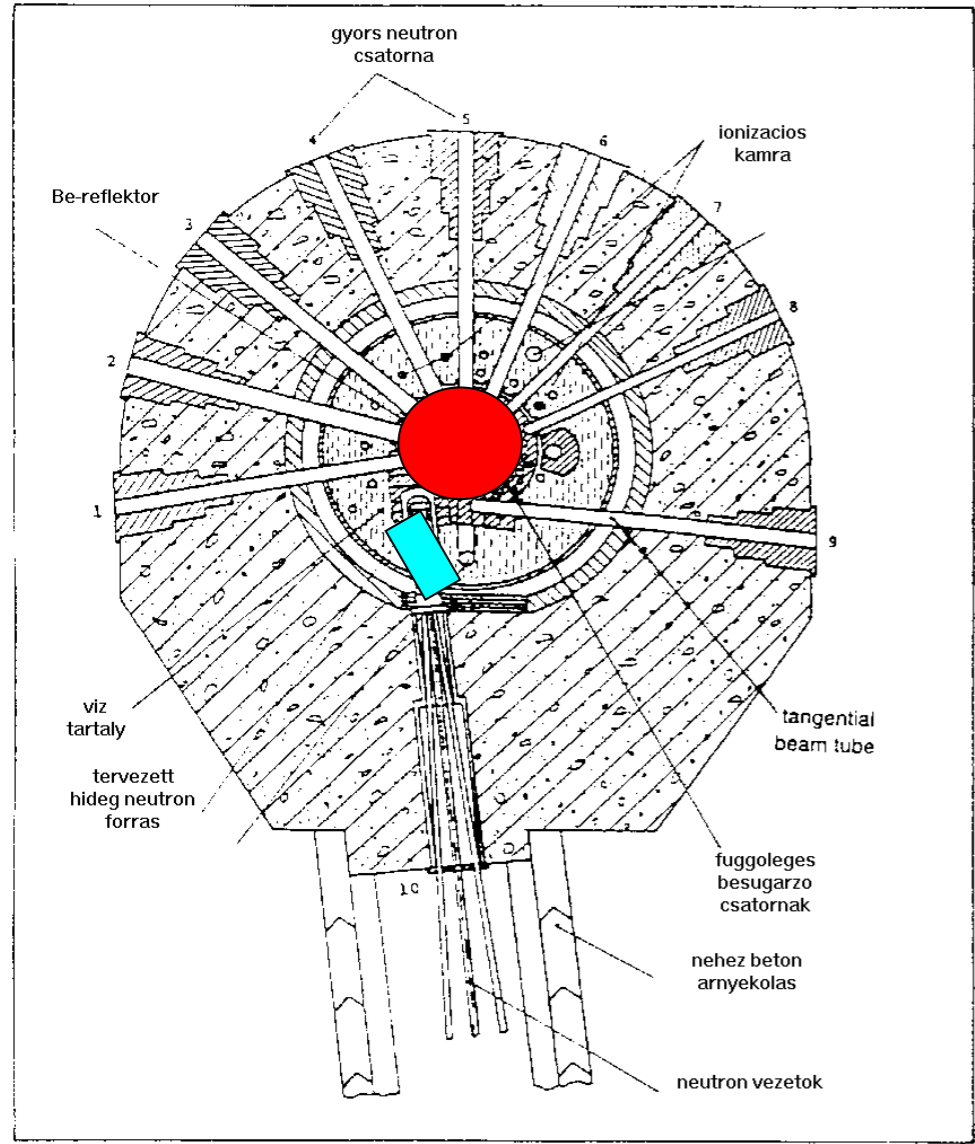






Unlike conventional irradiations, here we transfer the neutrons to the sample

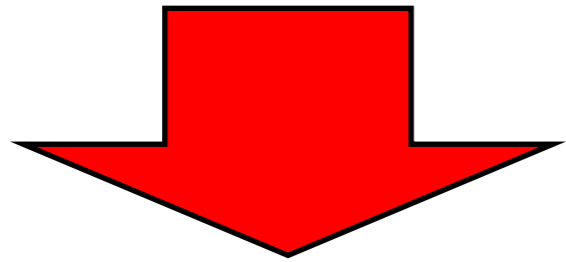




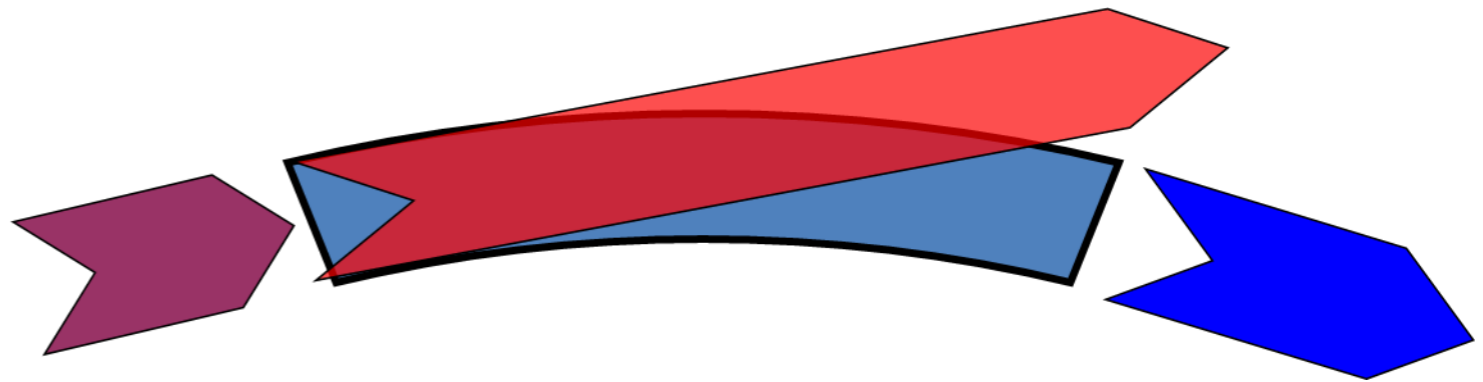
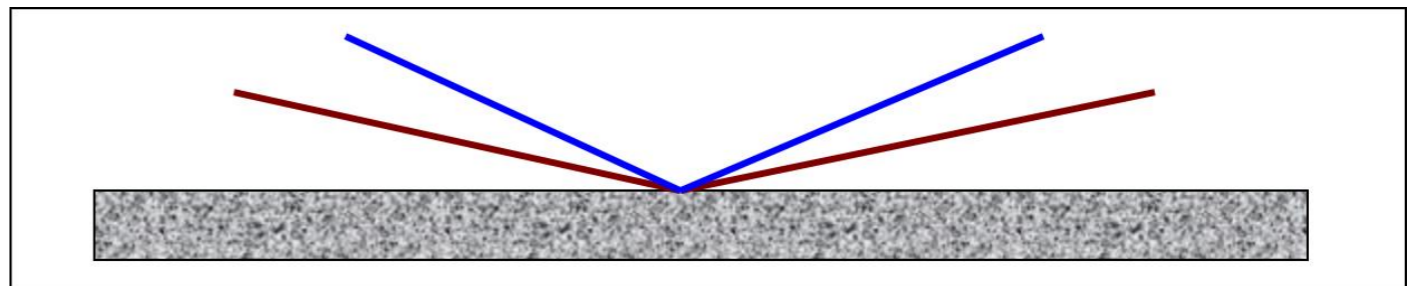
400 cm³, 20 K liquid H₂

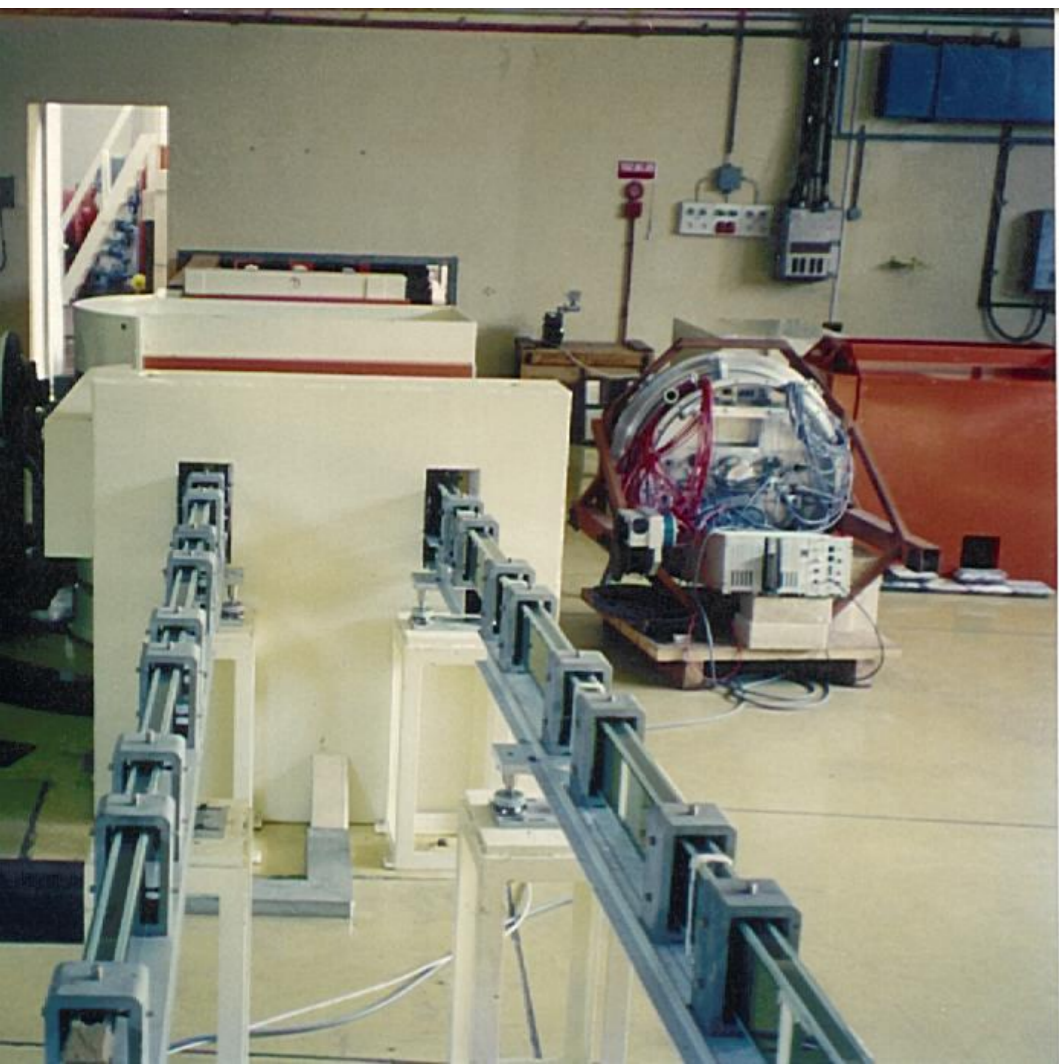


- Higher flux (neutron guides higher throughput)
- every nuclide behaves regularly
 - (follows the $1/v$ -law)
- every nuclide has higher cross section

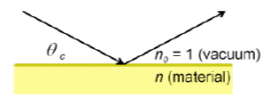


a higher reaction rate

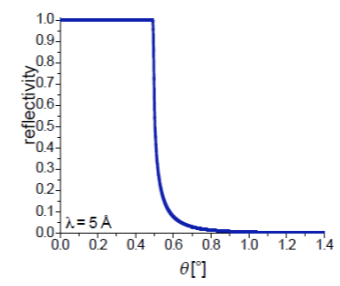




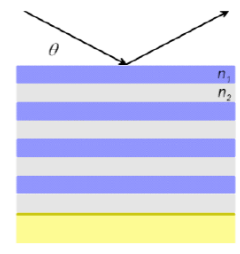
single mirror



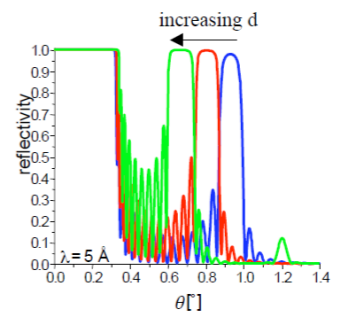
- ▶ refractive index $n < 1$
- ▶ total external reflection e.g. Ni $\theta_c = 0.1^\circ/\text{\AA}$



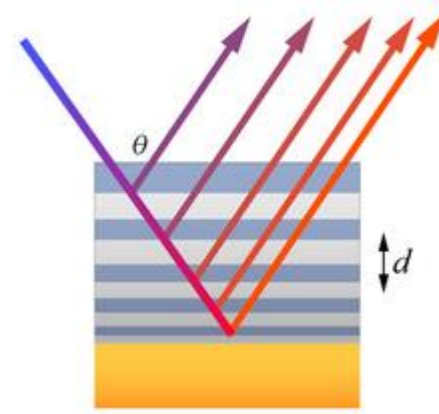
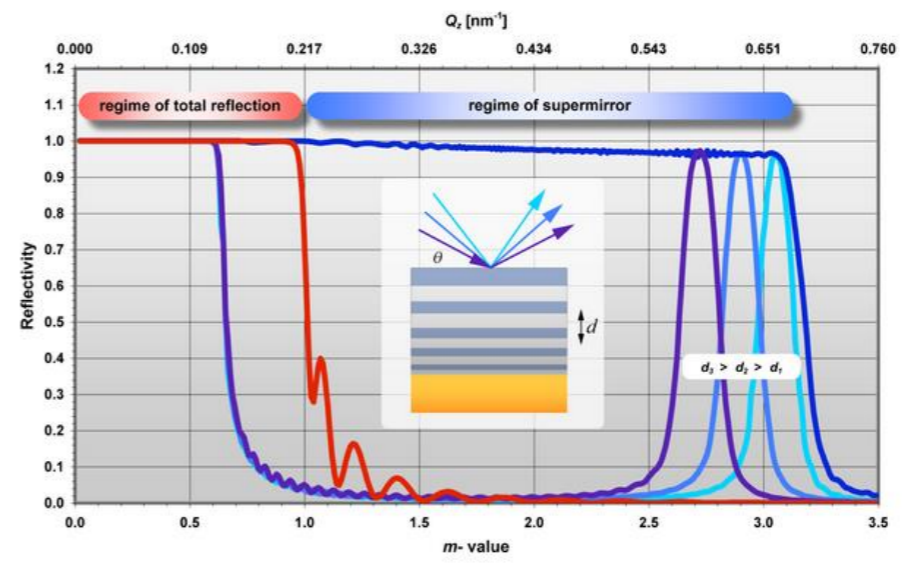
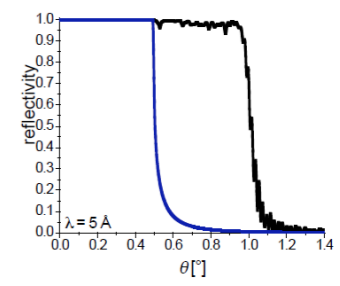
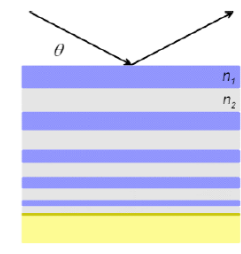
multilayer



$$\lambda = 2nd \sin \theta$$



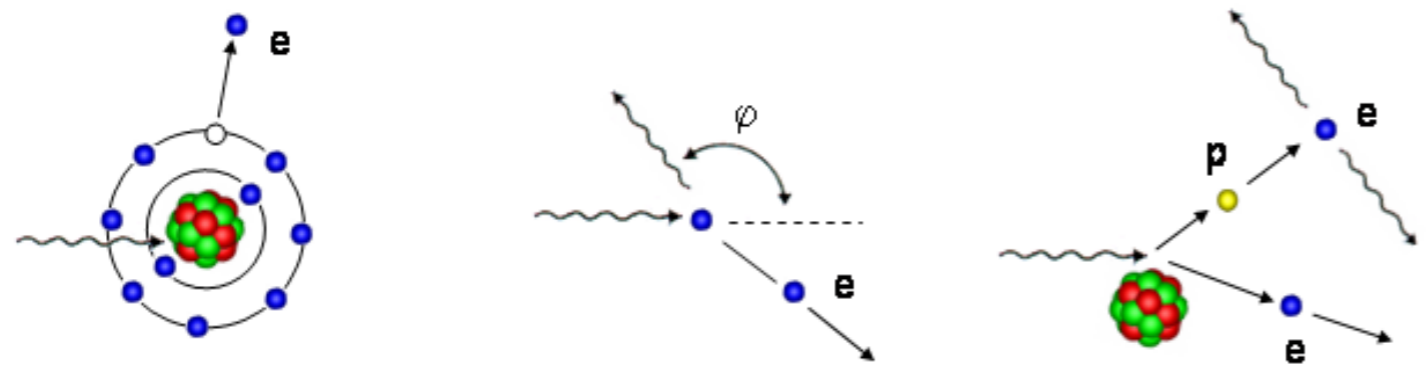
supermirror



- Ni or supermirror guides
- relatively small losses
- low background



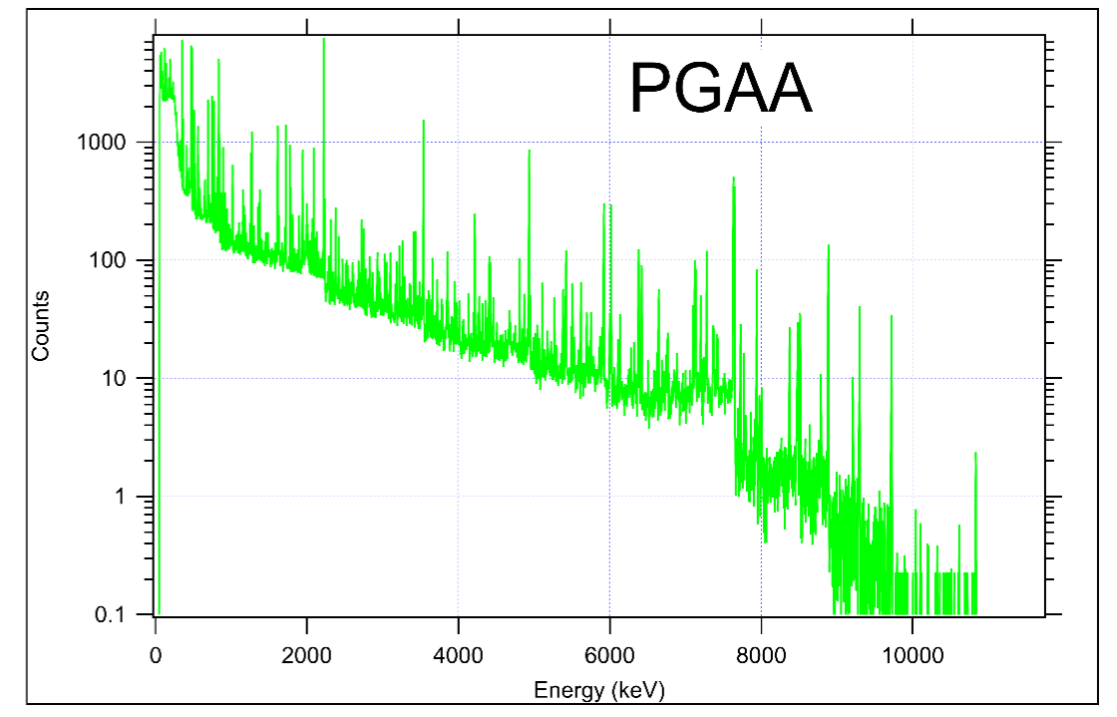
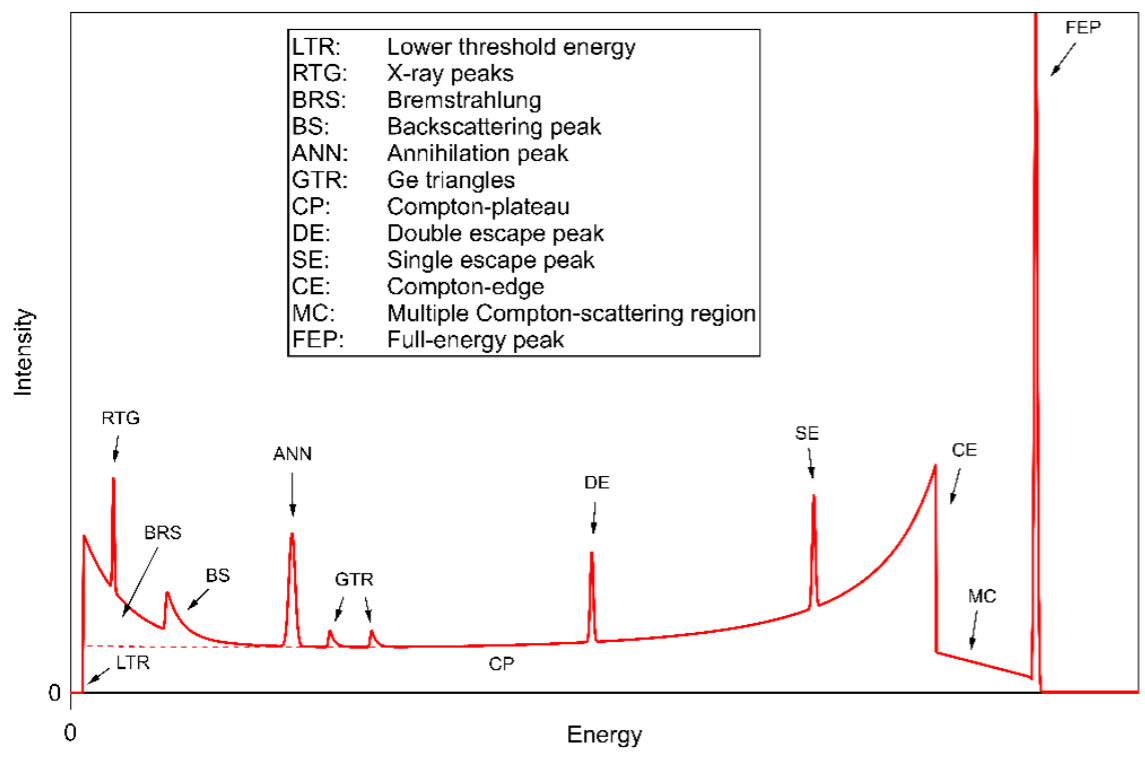
Three major types of interactions between gamma radiation and matter:



the photoelectric effect (left), the Compton-scattering (middle), and pair production (right).

(n,γ) spectra

- 45 keV to 12 MeV gamma energy range
- Complicated spectrum with hundreds of Gauss-like peaks
- Baseline increasing towards low energies
- Poisson statistics
- Peak positions -> identifying the elements
- Peak areas-> determining quantities

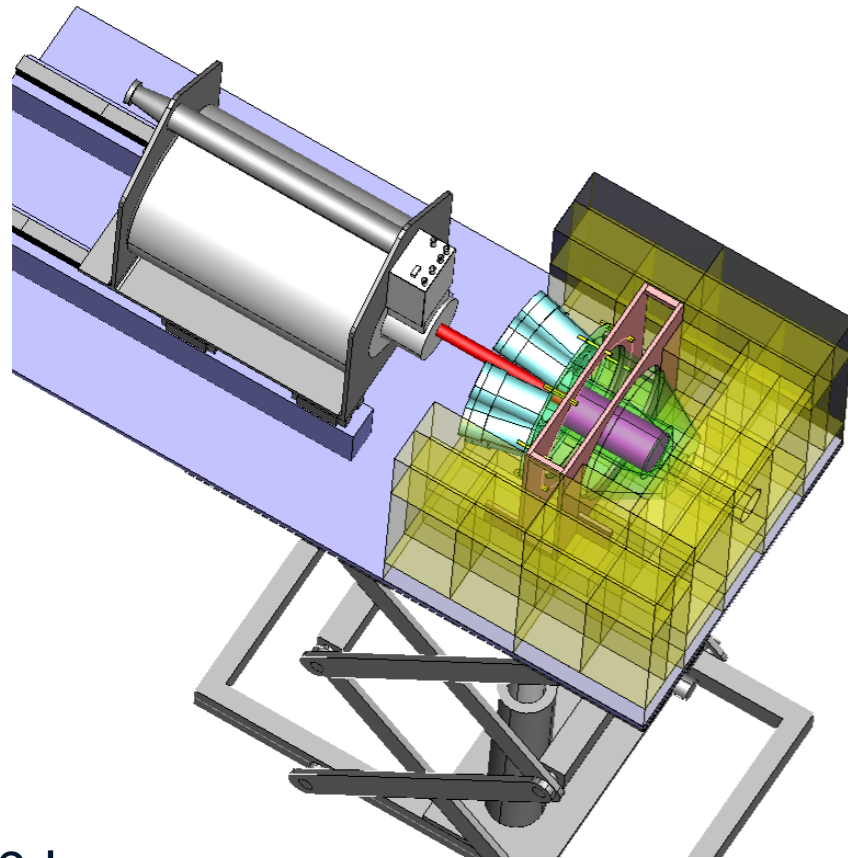




Aim: to reduce the background but not the peak!

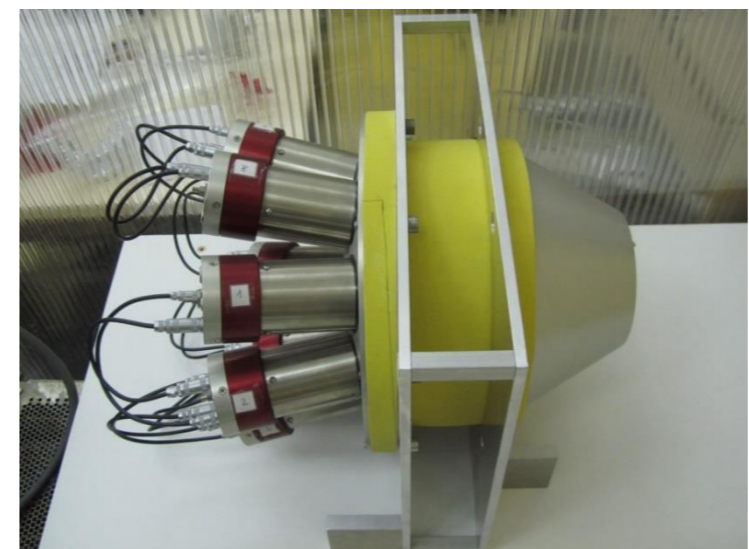
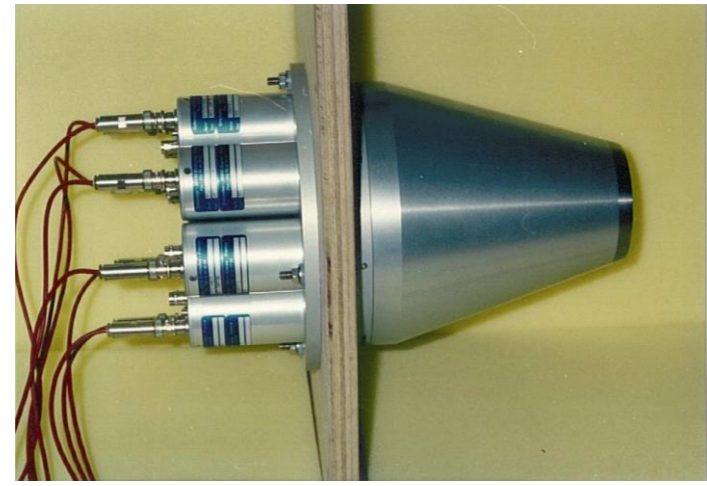
i.e. to selectively discard the events where interaction happened in both HPGe and suppressor, and keep all the events interacted only with HPGe

↓
BETTER
SIGNAL-TO-NOISE
RATIO



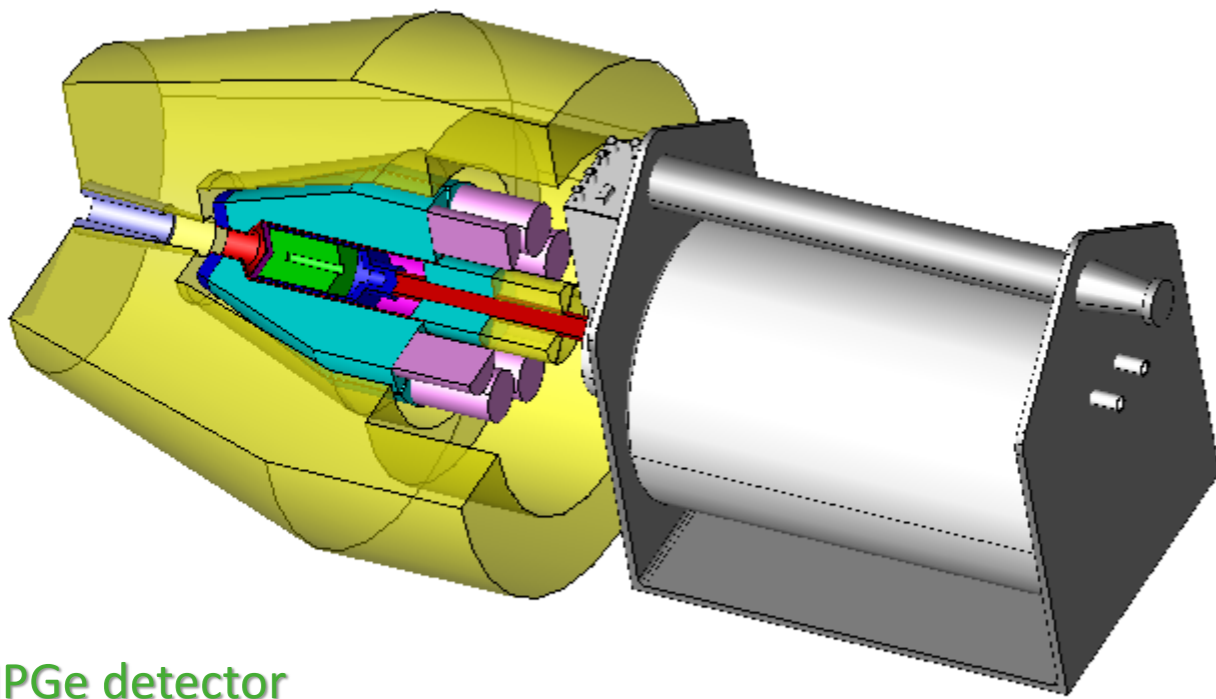
20-40 kg
 $\text{Bi}_4\text{GeO}_{12}$ (BGO)

Also reduces room background by more than 2 orders of magnitude





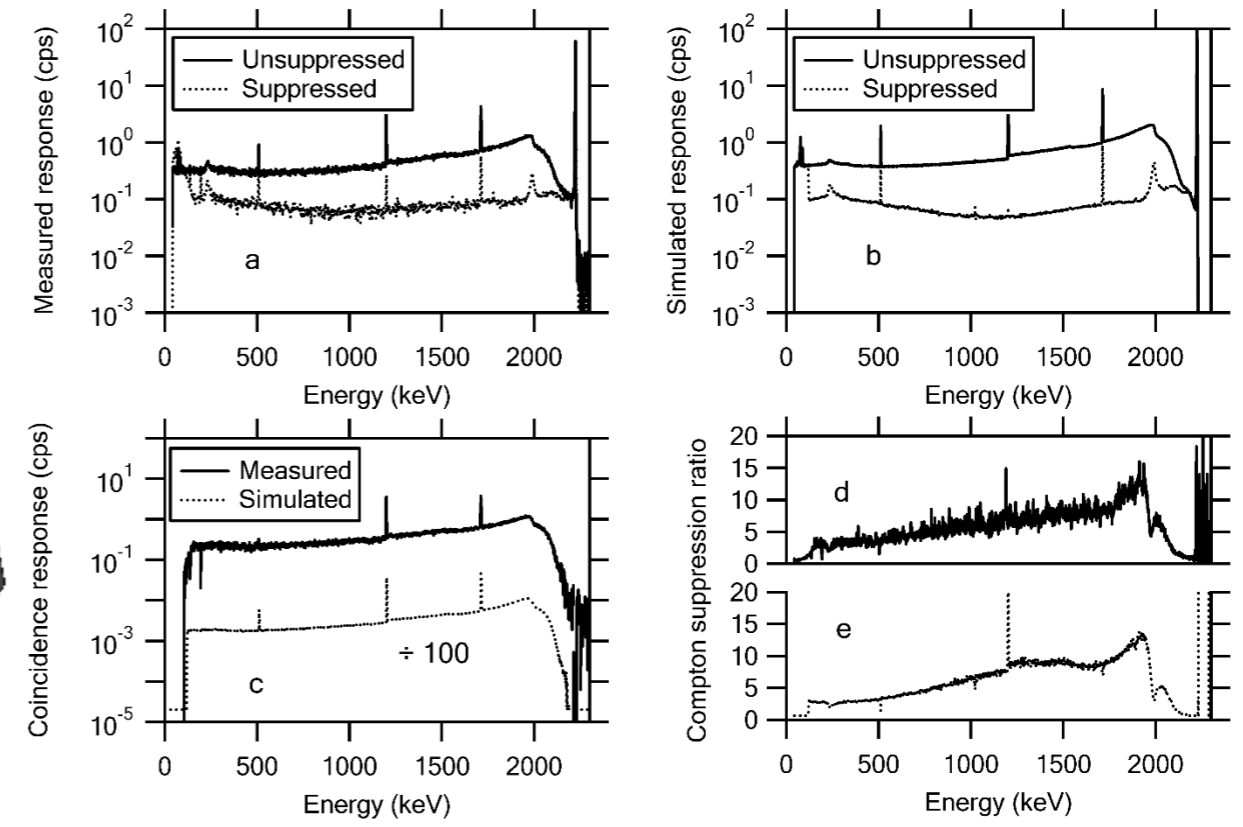
Central detector: high-purity Ge, due to best achievable energy resolution



HPGe detector

BGO Compton suppressor detector

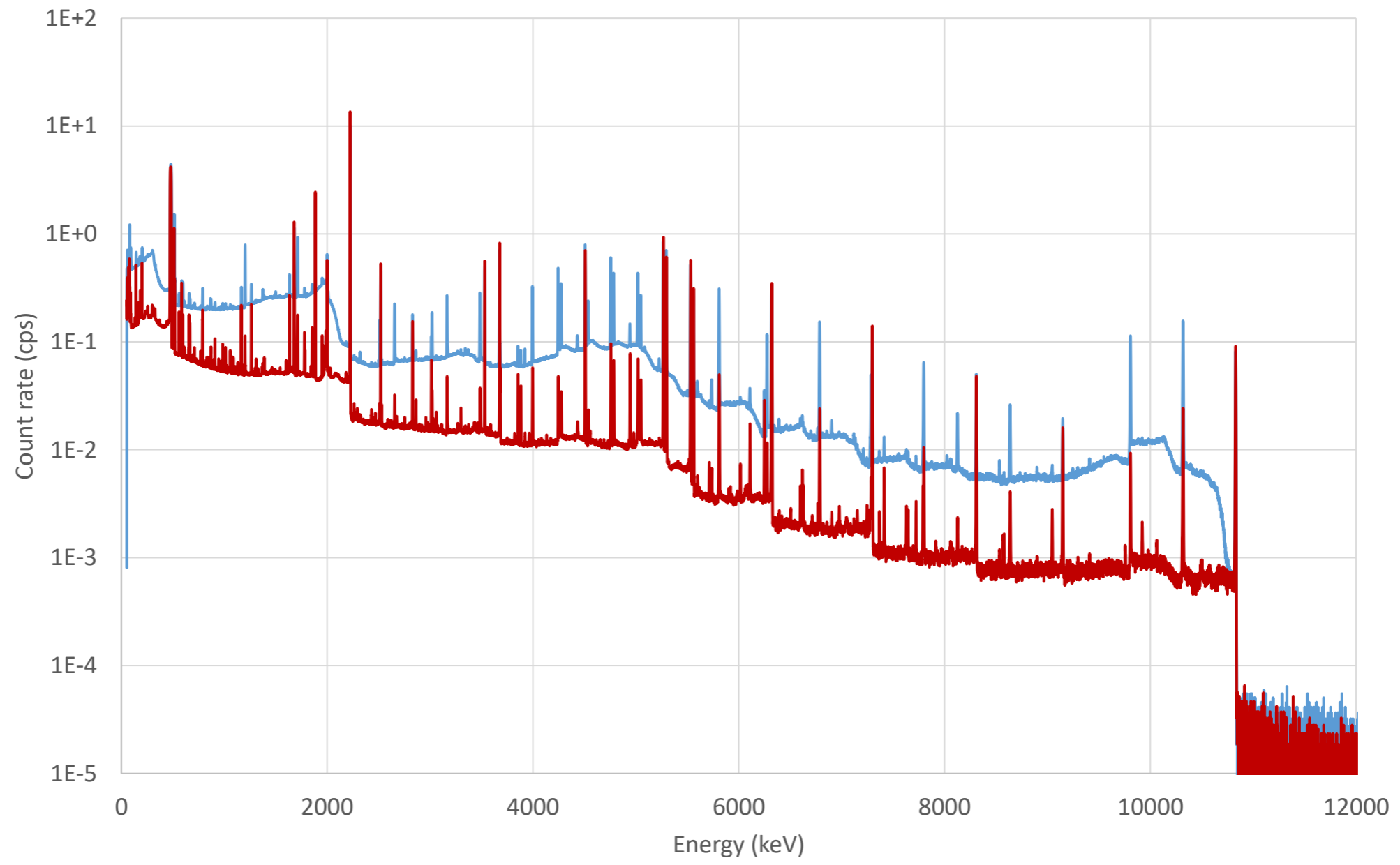
Lead shielding

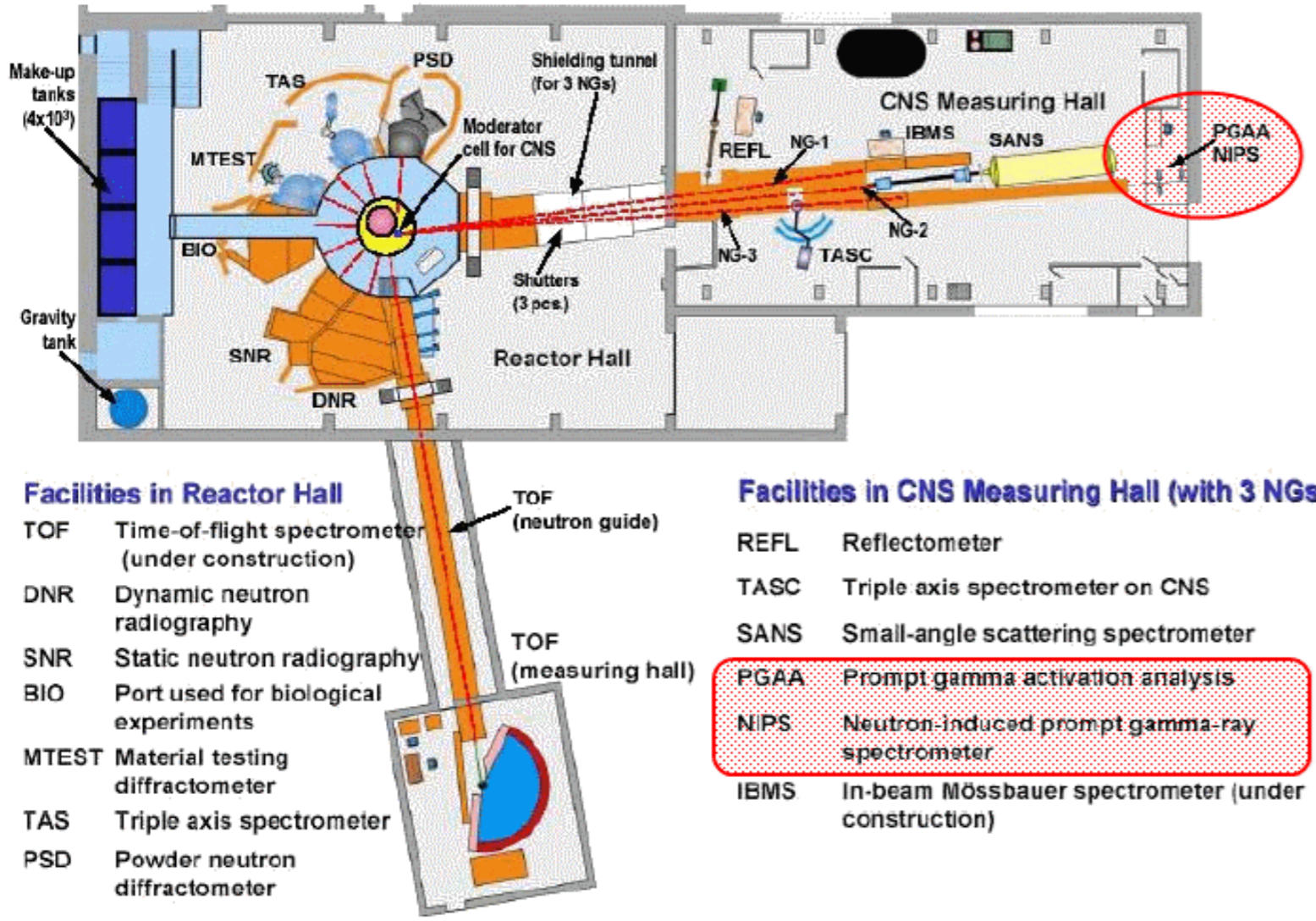


Detector response function for monenergetic gamma radiation (c.f. Compton scattering, pair production)

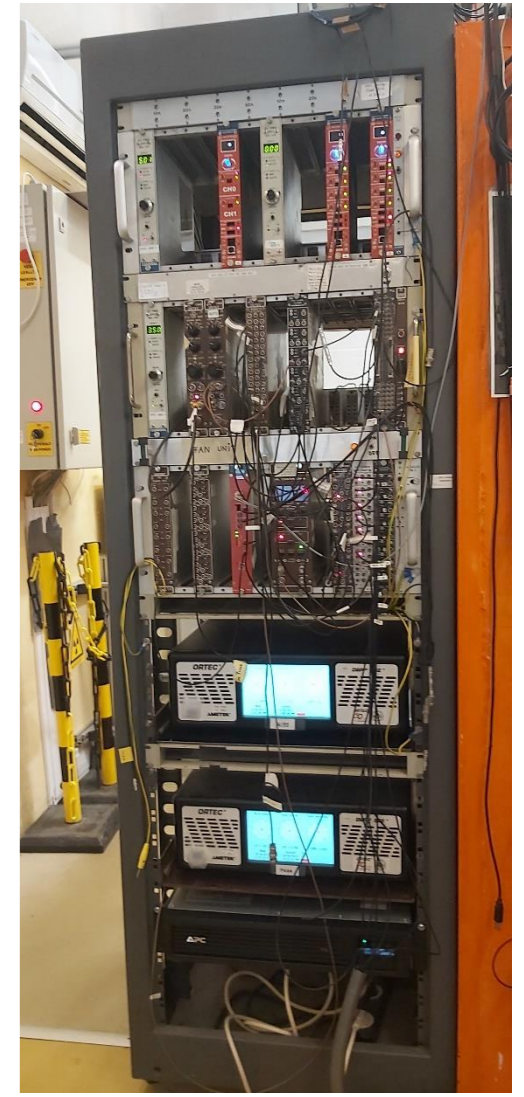


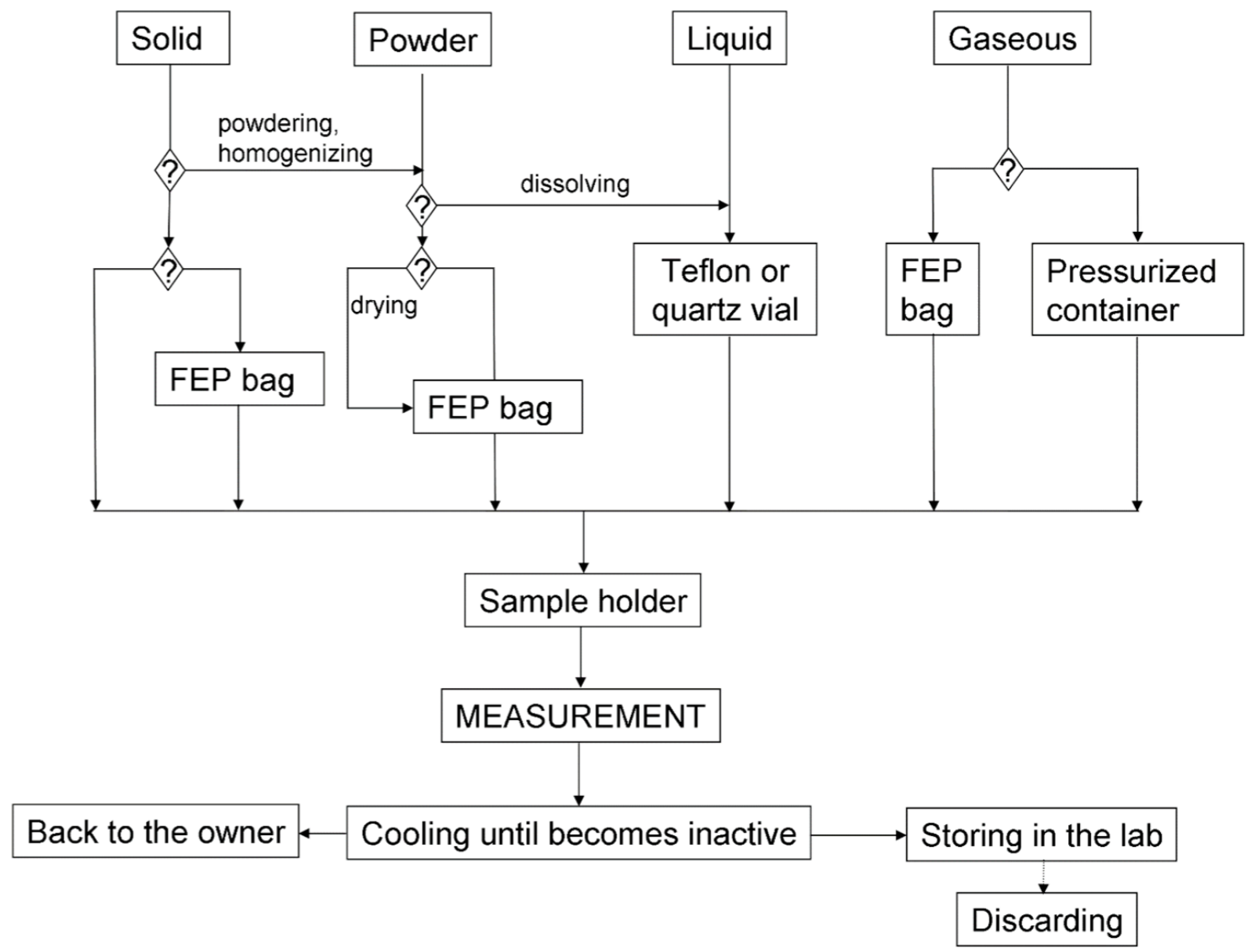
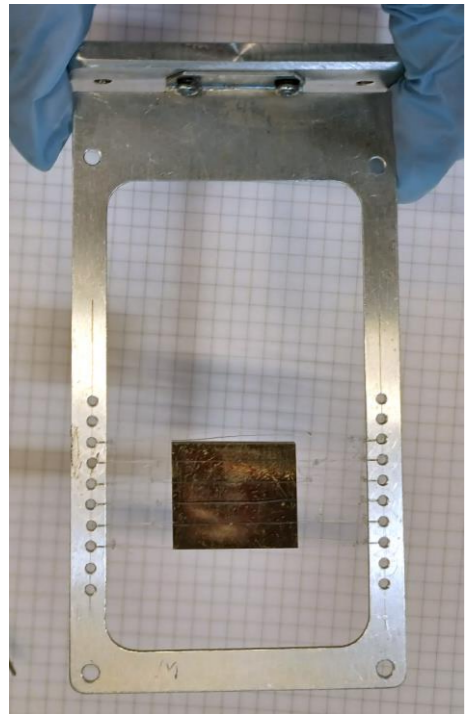
Unsuppressed vs. Compton-suppressed PGAA spectrum of Urea-D





- PGAA (prompt-gamma activation analysis spectrometer)
 - Increased productivity
 - Automation, reduce manpower
 - Higher throughput for small samples
- NIPS (neutron-induced prompt gamma spectrometer)
 - Specialization for bulky samples, position-sensitive applications
 - Combination with imaging system (NORMA)



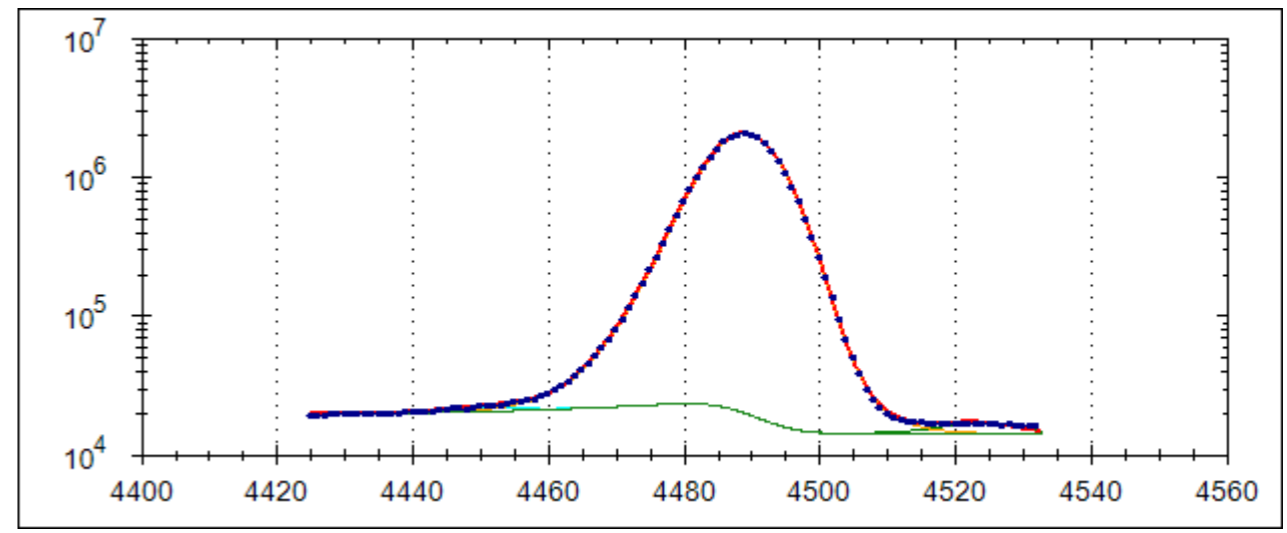
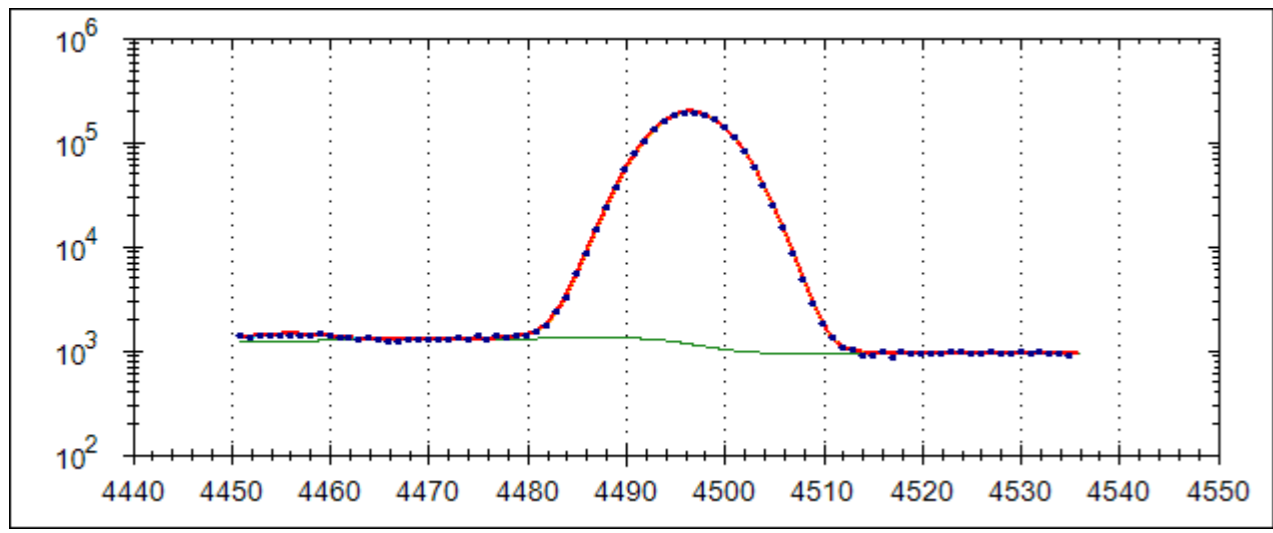


- **10 mg – 1 g sample mass**
- **Powder, solid -> Telfon bag**
- **Liquid -> Teflon vial**
- **Gas -> pressurized container**
- **Remains active only for a few hours (days) after irradiation**

Budapest Neutron Centre Centre for Energy Research

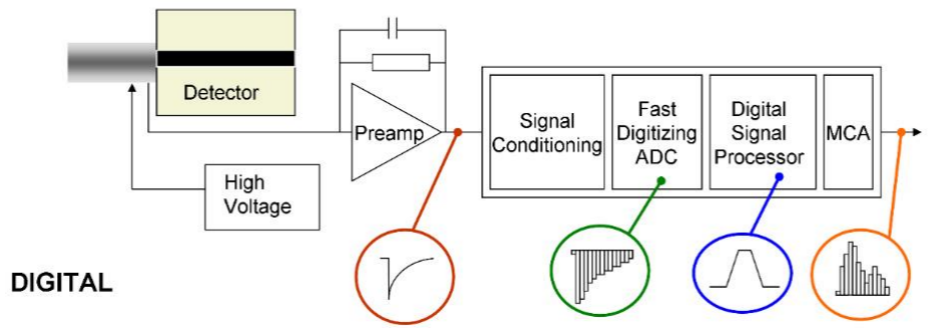
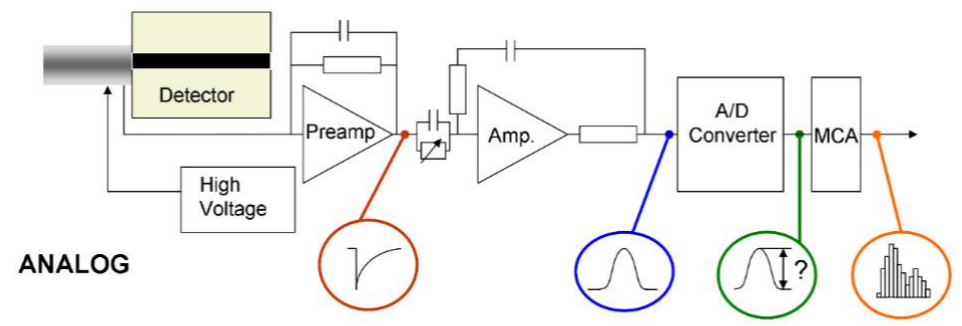
Calibration & evaluation methodology





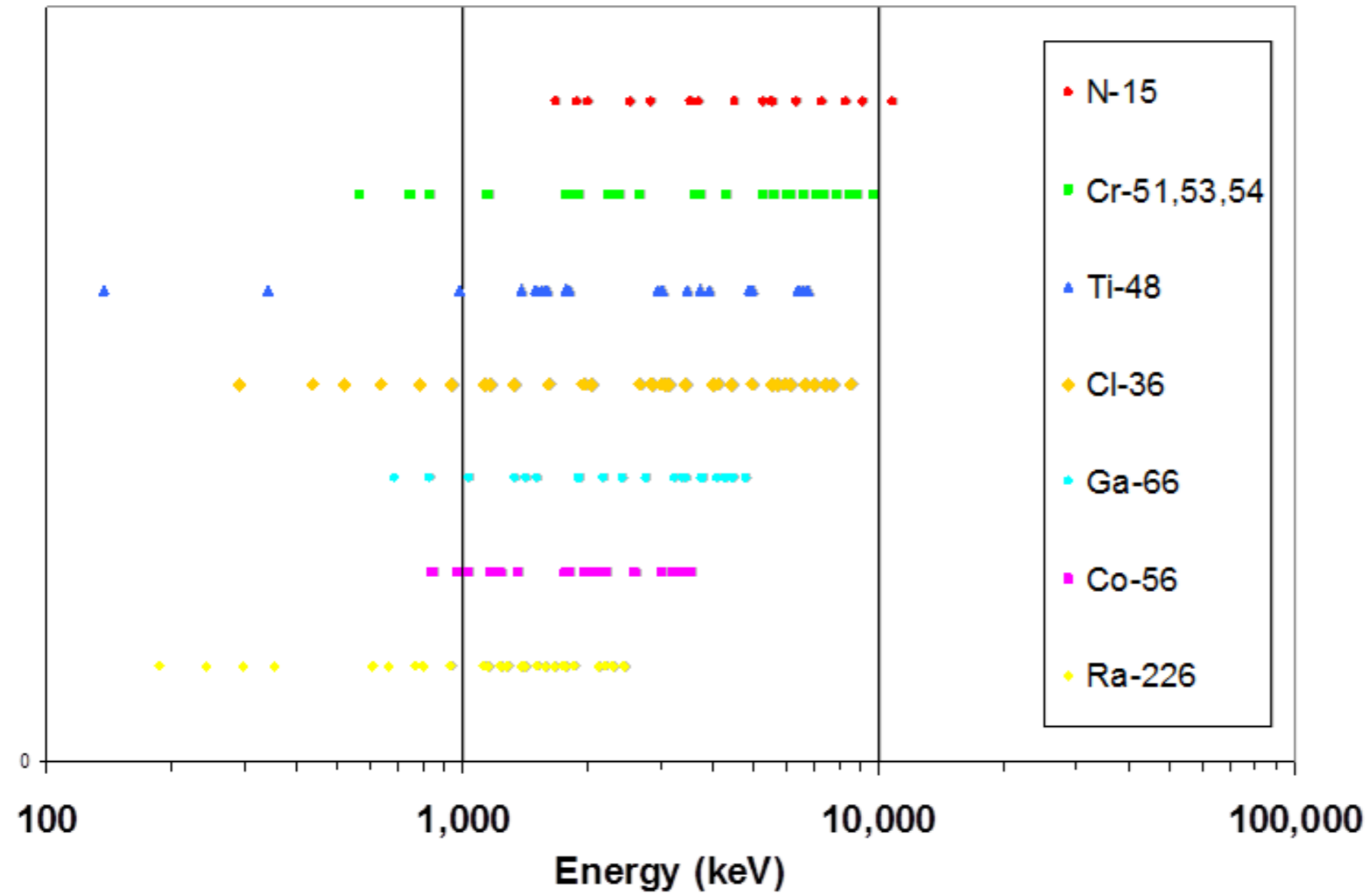
Optimum peak shape

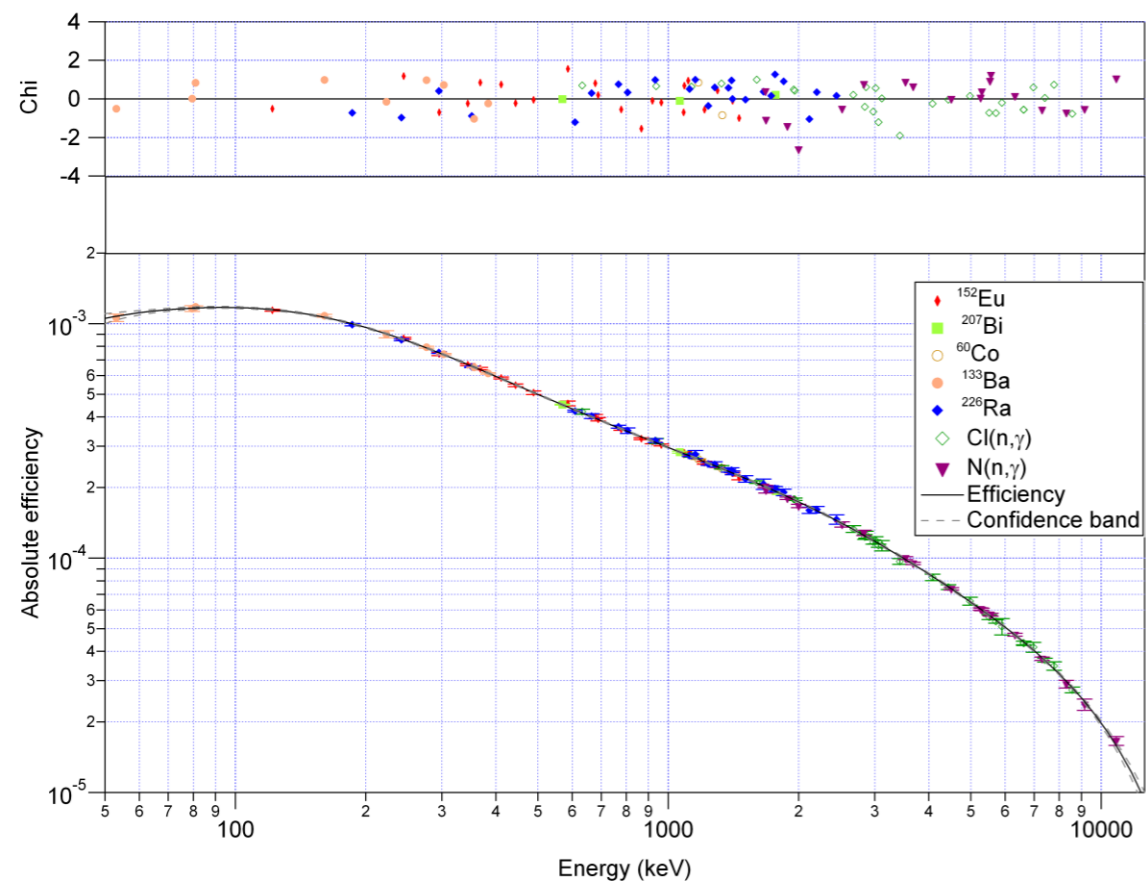
Distorted peak shape





Range of calibration sources





$$\varepsilon(1 \pm \delta\varepsilon) = \frac{A}{tP_\gamma a} \left(1 \pm \sqrt{(\delta A)^2 + (\delta P_\gamma)^2 + [(\delta a)^2]} \right)$$

A activity

P_γ emission probability

a source activity

Efficiency = detected events / emitted gamma photons

- Radioactive sources + well known (n,γ) reactions up to 11 MeV
- There is a correlation between two efficiency values if taken from the same curve: the correlation reduces the absolute uncertainty of efficiency ratios
- Efficiency ratio of two close-lying peaks tend to exact unity with no uncertainty



$$\frac{\varepsilon(E_1)}{\varepsilon(E_1)} \equiv 1 \quad \delta \frac{\varepsilon(E_1)}{\varepsilon(E_1)} \equiv 0$$

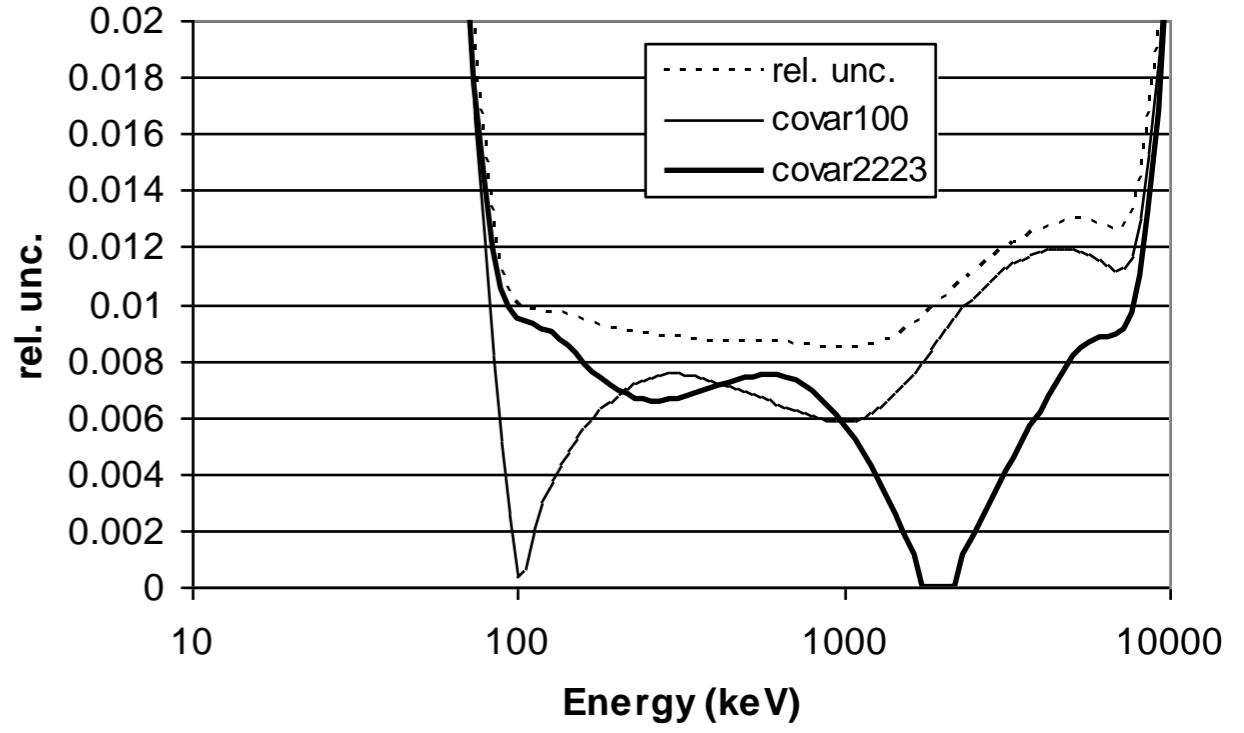
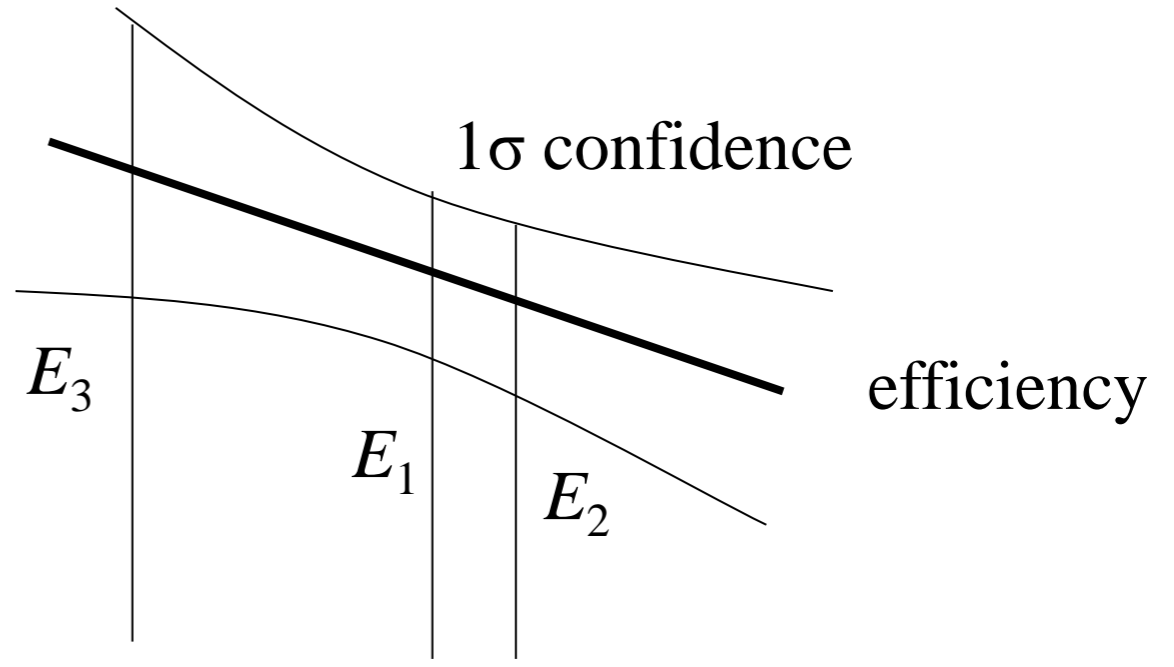
$$\delta \frac{\varepsilon(E_1)}{\varepsilon(E_2)} \approx 0$$

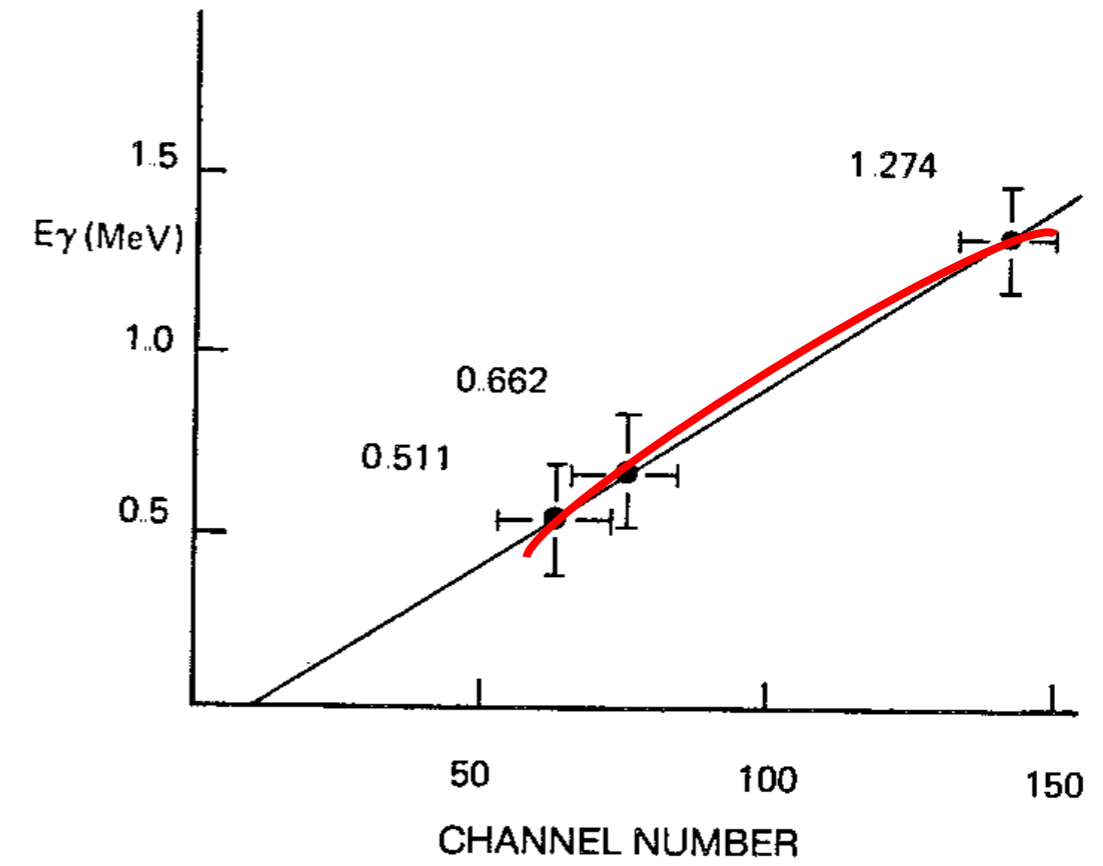
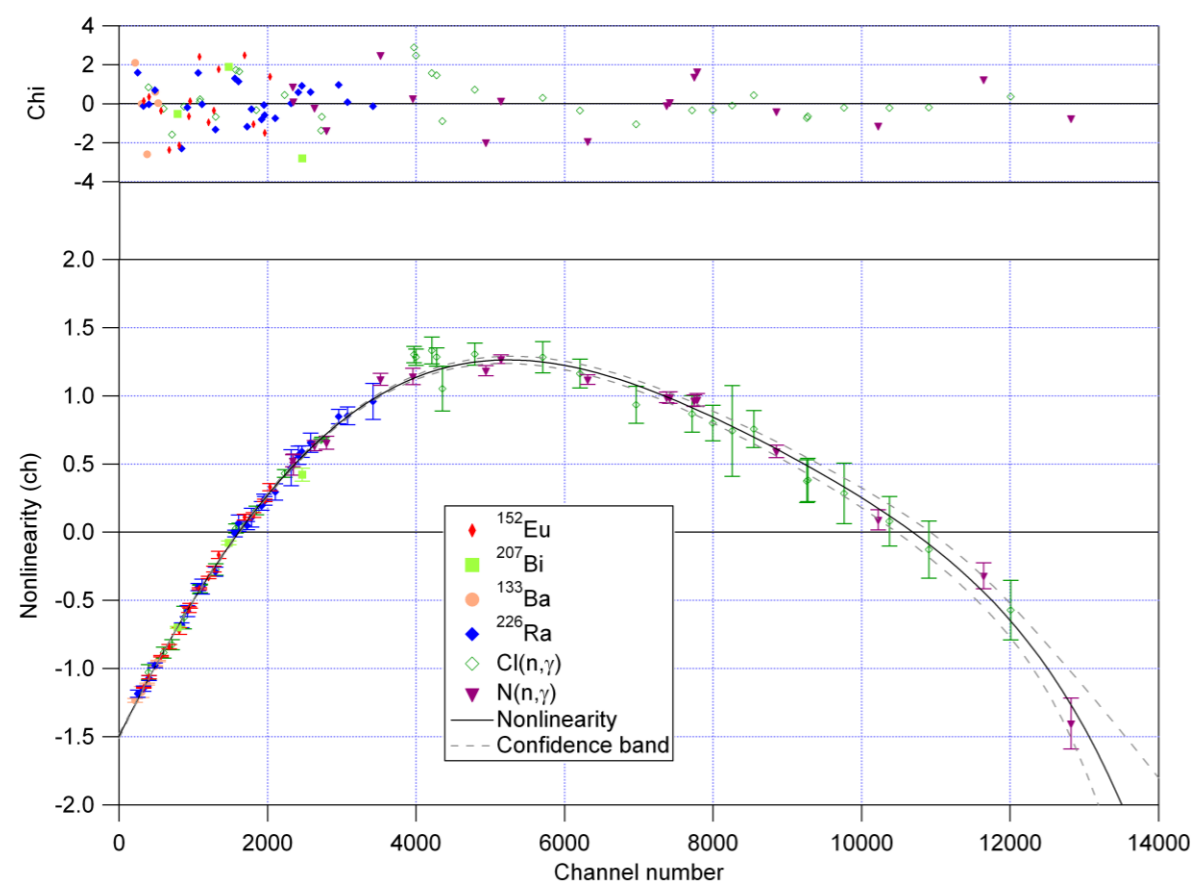
$$\delta \frac{\varepsilon(E_2)}{\varepsilon(E_3)} \approx \sqrt{(\delta\varepsilon(E_2))^2 + (\delta\varepsilon(E_3))^2}$$

The usual practice overestimates the uncertainty of the efficiency-correction, i.e. results in less precise cross-sections

$$\delta \frac{\varepsilon_c}{\varepsilon_x} = \sqrt{(\delta\varepsilon(E_x))^2 + (\delta\varepsilon(E_c))^2 - 2\delta\varepsilon(E_x, E_c)}$$

Belgya, T. (2014). Uncertainty calculation of functions of γ -ray detector efficiency and its usage in comparator experiments. *J Radioanal Nucl Chem*, 300(2), 559–566.

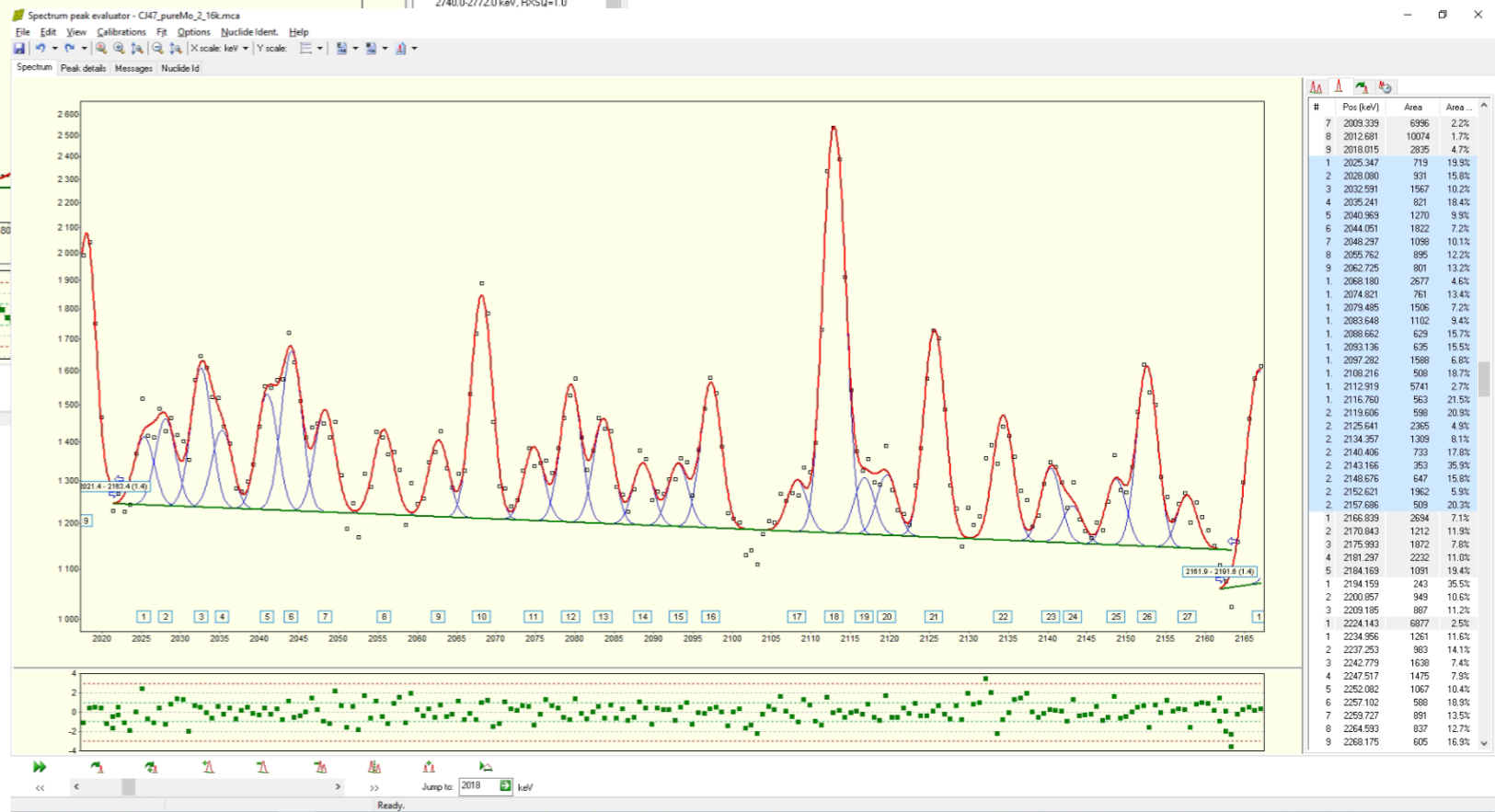
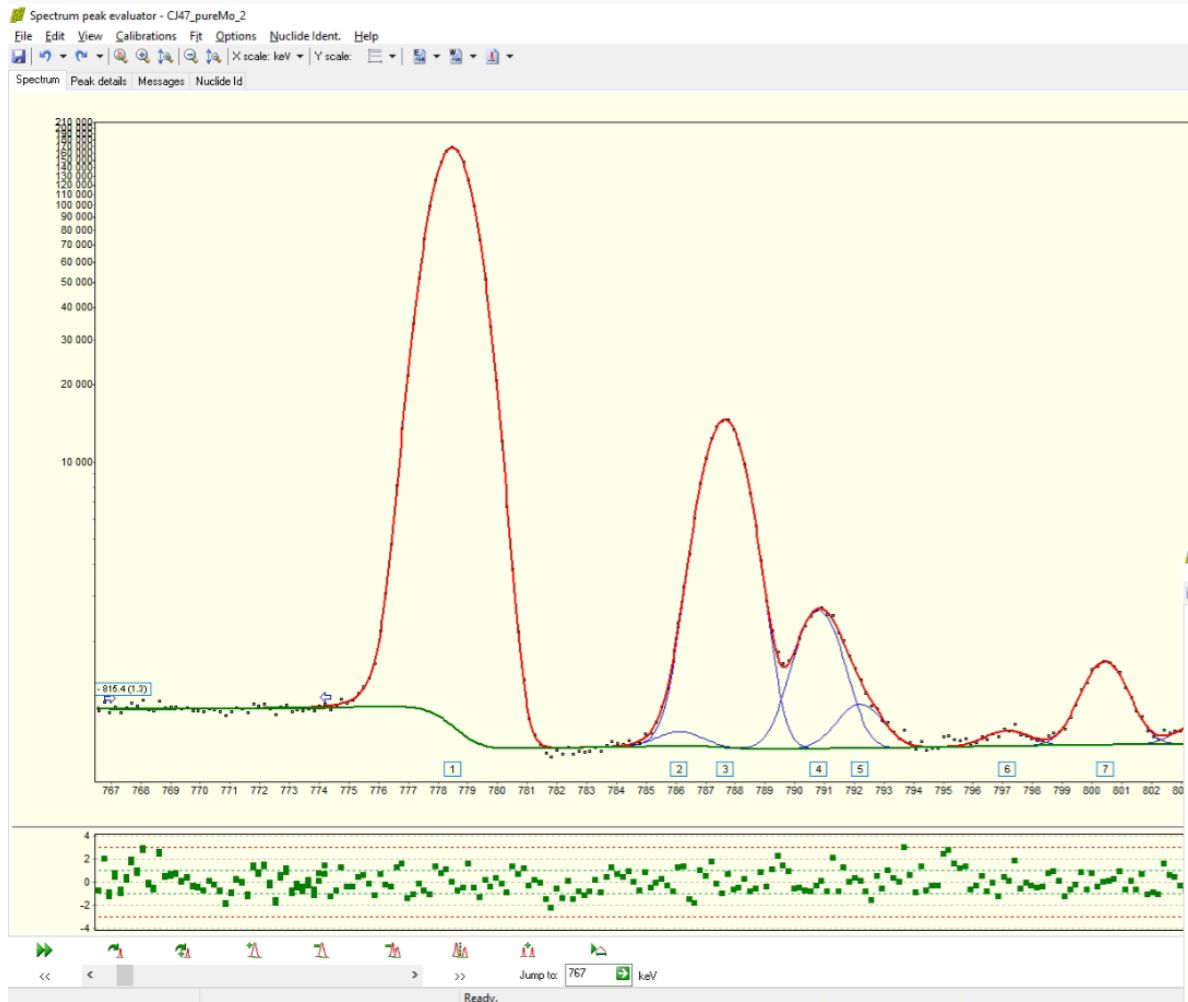




Nonlinearity is to compensate for a small, but systematic bias in the linear energy-channel correspondence

Calculated for two-point linear energy calibration, where NL at the calibration energies are set to zero not to influence the literature energy value

Fazekas, B., et al. (1999). A new method for determination of gamma-ray spectrometer non-linearity. *Nuclear Instruments & Methods A*, 422(1-3), 469-473.



Budapest Neutron Centre Centre for Energy Research

Determination of cross-sections
using a comparator





- Comparator-based standardization is the procedure, where we obtain the cross-section of an element or isotope of interest by direct comparison to the signal of an other reference element or isotope, whose nuclear parameters are accurately known
- This reduces or eliminates the influence of many experimental parameters that are difficult to control
- Provides unbiased and precise values, and can be adjusted should the reference value change
- If done systematically, can be used in form of a database



- Ultimate comparator:
 - H line at 2223.255 keV with 0.3326(7) barn (=0.2% unc!)
- Primary comparators: C, N, O, F, S, Cl, Fe (Au)
- One-, or two-step standardization
- Unbroken chain of traceability to H cross-section
- This ensures internal consistency of a measurement series

$$\cancel{\sigma_{\gamma,x} = \frac{n_c \frac{A_x}{\varepsilon(E_x)}}{n_x \frac{A_c}{\varepsilon(E_c)}} \sigma_{\gamma,c} = \frac{n_c A_x \varepsilon(E_c)}{n_x A_c \varepsilon(E_x)} \sigma_{\gamma,c}}$$



- Elemental spectra: to obtain ...
 - Relative positions
 - Relative intensities
- Energy calibration: to absolutize energy scale
 - 2 energies from the 2-point E-calibration
 - Non-linearity correction
- Standardization: to absolutize intensity scale
 - efficiency ratios
 - Pure, stoichiometric compounds or mixtures
- Good comparator:
 - Its nuclear data are known to high precision
 - has a peak close to the peak of interest in energy
 - has similar partial gamma-ray production cross-section not to saturate the counting system

Révay, Z., & Molnár, G. L. (2003). Standardisation of the prompt gamma activation analysis method. *Radiochimica Acta*, 91(6), 361–369



$$\sigma_x(1 \pm \delta\sigma_x) = \frac{A_x \varepsilon(E_c) n_c}{A_c \varepsilon(E_x) n_x} \sigma_c \left(1 \pm \sqrt{(\delta A_x)^2 + (\delta A_c)^2 + \left(\delta \frac{\varepsilon(E_c)}{\varepsilon(E_x)}\right)^2 + (\delta\sigma_c)^2} \right) =$$

$$= \frac{A_x \varepsilon(E_c) n_c}{A_c \varepsilon(E_x) n_x} \sigma_c \left(1 \pm \sqrt{(\delta A_x)^2 + (\delta A_c)^2 + (d\varepsilon(E_x))^2 + (d\varepsilon(E_c))^2 - 2d\varepsilon(E_x, E_c) + (\delta\sigma_c)^2} \right)$$

n stoichiometric coeff. – accurate, no unc assigned

$\sigma_H = 0.3326(7)$ barn – ultimate comparator

Sears, V. F. (1992). Neutron Scattering Lengths and Cross Sections. *Neutron News*, 3(3), 26–37.

- Unc can be reduced by:
 - Increasing the counts in the peaks (A_x and A_c)
 - Reducing the uncertainty of the efficiency curve
 - Using efficiency ratio rather than ratios of efficiencies
 - Using a comparator with very well known cross-section

Révay, Zs. (2006). Calculation of uncertainties in prompt gamma activation analysis. *Nuclear Instruments & Methods A* 564(4–6), 688–697.



Two separate measurement, but using the same beam and detector

Example: Cl vs H, and Na vs Cl

$$\begin{aligned} \sigma_y(1 \pm \delta\sigma_y) &= \frac{A'_y [\varepsilon(E_x)] n'_x}{A'_x \varepsilon(E_y) n'_y} \frac{A_x \varepsilon(E_c) n_c}{A_c [\varepsilon(E_x)] n_x} \times \\ &\times \left(1 \pm \sqrt{(\delta A'_y)^2 + (\delta A'_x)^2 + (\delta A_x)^2 + (\delta A_c)^2 + (\delta\varepsilon(E_y))^2 + (\delta\varepsilon(E_c))^2 - 2\delta\varepsilon(E_y, E_c)} + (\delta\sigma_c)^2 \right) = \\ &= \frac{A'_y \varepsilon(E_x) n'_x}{A'_x \varepsilon(E_y) n'_y} \sigma_x \times \\ &\times \left(1 \pm \sqrt{(\delta A'_y)^2 + (\delta A'_x)^2 + (\delta\sigma_x)^2 - (\delta\varepsilon(E_x))^2 + 2\delta\varepsilon(E_x, E_c) + (\delta\varepsilon(E_y))^2 - 2\delta\varepsilon(E_y, E_c)} \right) \end{aligned}$$

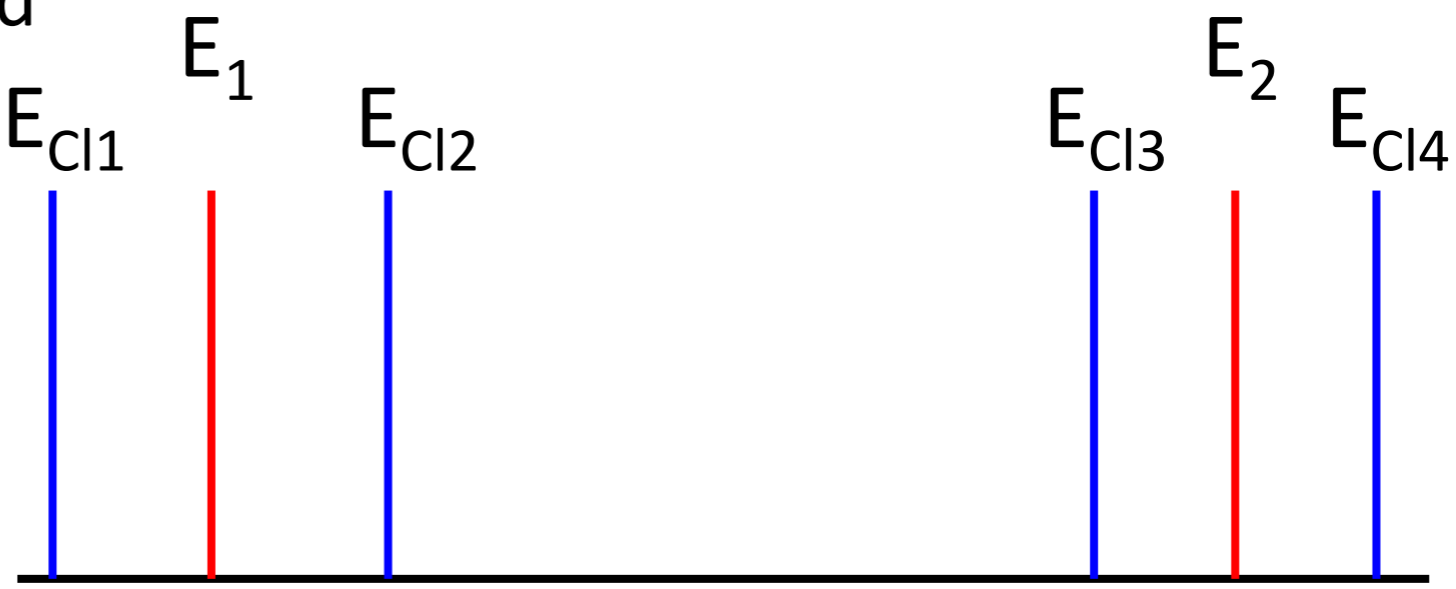
$$\begin{aligned} \frac{\sigma_1}{\sigma_2} \left(1 \pm \delta \frac{\sigma_1}{\sigma_2} \right) &= \frac{A_1/A_c \varepsilon(E_2) n_c/n_1}{A'_2/A'_c \varepsilon(E_1) n'_c/n'_2} \times \\ &\times \left(1 \pm \sqrt{(\delta A_1)^2 + (\delta A_c)^2 + (\delta A'_2)^2 + (\delta A'_c)^2 + (\delta\varepsilon(E_1))^2 + (\delta\varepsilon(E_2))^2 - 2\delta\varepsilon(E_1, E_2)} \right) = \\ &= \frac{\sigma_1}{\sigma_2} \left(1 \pm \sqrt{(\delta\sigma_1)^2 + (\delta\sigma_2)^2 - 2(\delta\varepsilon(E_c))^2 + 2\delta\varepsilon(E_1, E_c) + 2\delta\varepsilon(E_2, E_c) - 2(\delta\sigma_c)^2} \right) \end{aligned}$$



- Energy difference method: interpolation based on two neighboring reference peaks, where precise literature energy values are available
- Crystal spectrometer data for ^{35}Cl

Krusche, B., Lieb, K. P., Daniel, H., von Egidy, T., Barreau, G., Börner, H. G., Brissot, R., Hofmeyr, C., & Rascher, R. (1982). Gamma-ray energies and ^{36}Cl level scheme from the reaction $^{35}\text{Cl}(n,g)$. *Nuclear Physics - Section A*, 386, 245–268.

- The target is measured in presence of Cl
- Non-linearity is also considered





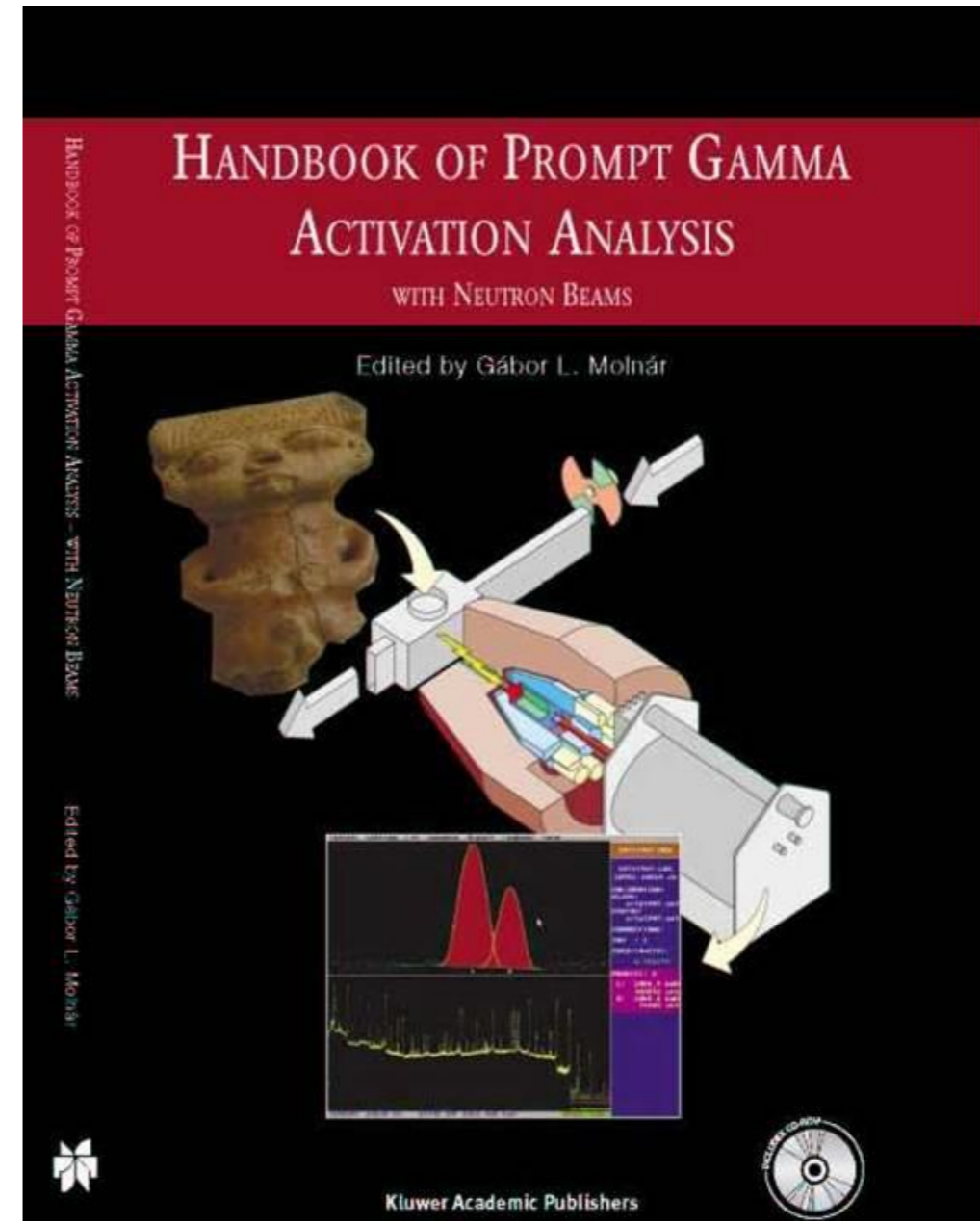
Consistency test for the 1884 keV N line vs H, Cl, S



	Sample	Peak area ratio $\times n_H/n_N$	Unc. (%)	Weighted average	χ	Unc. (%)	Eff ratio ϵ_N/ϵ_H	σ_γ (barn)	Syst. unc. (%)	Total unc. (%)
1	piridine	0,05033	0,5	0,05018	1,5	0,32	1,1456	0,01457	0,21	0,38
2	(NH₄)₂SO₄	0,05106	0,9		2,4					
3	NH ₄ NO ₃	0,05029	0,6		1,1					
4	NH ₄ NO ₃	0,05009	1,1		0,23					
5	NH ₄ NO ₃	0,04998	0,7		0,06					
6	NH ₄ Cl	0,04763	2,4		-1,9					
7	melamine	0,05000	0,3	0,05000		0,3	1,1456	0,01452	0,21	0,37



Z	EI	A	MW	#	E	dE	σ	d σ %	RI	Area	cps/g
1	H	1	1.01	1	2223.259	0.019	0.3326	0.2	100.00	100.00	64.183
1	H	2	1.01	2	6250.204	0.098	0.000492	5.0	0.15	5.00	0.0286
3	Li	6	6.94	5	477.586	0.050	0.001399	5.9	3.52	10.14	0.1218
3	Li	7	6.94	2	980.559	0.046	0.004365	5.1	10.97	18.74	0.2251
3	Li	7	6.94	3	1051.817	0.048	0.004364	5.1	10.97	17.83	0.2141
3	Li	7	6.94	1	2032.310	0.070	0.0398	5.0	100.00	100.00	1.2007
3	Li	6	6.94	6	6769.633	0.263	0.001354	6.5	3.40	0.84	0.0101
3	Li	6	6.94	4	7246.800	0.275	0.002106	8.4	5.29	1.17	0.014
4	Be	9	9.01	4	853.631	0.011	0.00165	8.9	26.69	100.00	0.0723
4	Be	9	9.01	3	2590.014	0.025	0.00188	8.9	30.41	49.08	0.0355
4	Be	9	9.01	2	3367.484	0.035	0.002924	8.9	47.30	58.96	0.0427
4	Be	9	9.01	5	3443.421	0.036	0.000993	8.9	16.06	19.54	0.0141
4	Be	9	9.01	6	5956.602	0.092	0.000146	9.1	2.36	1.41	0.001
4	Be	9	9.01	1	6809.579	0.099	0.006181	9.0	100.00	48.52	0.0351
5	B	10	10.81	1	477.600	5.000	712.5	0.3	100.00	100.00	39806
6	C	12	12.01	2	1261.708	0.057	0.00123	2.7	45.58	100.00	0.0306
6	C	12	12.01	3	3684.016	0.069	0.001175	3.5	43.53	38.02	0.0116
6	C	12	12.01	1	4945.302	0.066	0.002699	2.9	100.00	60.55	0.0186
7	N	14	14.01	22	583.567	0.031	0.000429	3.3	1.81	6.93	0.0159
7	N	14	14.01	12	1678.244	0.029	0.006254	1.5	26.34	47.15	0.1085
7	N	14	14.01	18	1681.174	0.043	0.001296	2.7	5.46	9.76	0.0225
7	N	14	14.01	21	1853.944	0.052	0.000474	4.5	2.00	3.31	0.0076
7	N	14	14.01	5	1884.853	0.031	0.0145	1.3	61.07	100.00	0.2301
7	N	14	14.01	24	1988.532	0.077	0.000294	5.8	1.24	1.94	0.0045
7	N	14	14.01	15	1999.693	0.032	0.003208	1.7	13.51	21.12	0.0486
7	N	14	14.01	13	2520.446	0.039	0.004246	1.8	17.88	22.98	0.0529





- Evaluation: to scrutinize the raw measured data, judge their quality, potential biases, reject outliers and specify a cross-section value that is true and precise
- The raw measurement data are checked for consistency against nuclear principles (e.g. conservation of energy)
- E.g. sum of (n,g) intensities and radioactive decay gammas (after correcting with the branching ratio) are dependent

- Cross-checked with other measurements

$$\chi_{E,i} = \frac{E_i - E_{lib,i}}{\sqrt{(\Delta E_i)^2 + (\Delta E_{lib,i})^2}}$$

- Different methodologies might have different systematic errors, help to reveal bias
- Simply averaging a good and a bad value is not a good practice
- EGAF: Evaluated Gamma Activation File by Berkeley National Lab, USA (R.B. Firestone, A. Hurst)
- Available on-line at IAEA NDS (<https://www-nds.iaea.org/pgaa/egaf.html>) or as a python script (pyEGAF, https://github.com/AaronMHurst/python_egaf)

A.M. Hurst, R.B. Firestone, E.V. Chimanski: pyEGAF: An open-source python library for the evaluated Gamma-ray activation file, Nucl. Instr. Meth A 2023 DOI: [10.1016/j.nima.2023.168715](https://doi.org/10.1016/j.nima.2023.168715)

pyEGAF

https://github.com/AaronMHurst/python_egaf

This project is a Python package enabling interaction, manipulation, and analysis of thermal-neutron capture gamma-ray data from the Evaluated Gamma-ray Activation File (EGAF) library [1], [2]. The EGAF library is a database of γ -ray energies and their corresponding partial γ -ray cross sections from thermal-neutron capture measurements carried out with a guided neutron beam at the Budapest Research Reactor for 245 isotopes encompassing measurements of natural elemental samples for targets from Z = 1-83, 90, and 92, except for Tc (Z = 43) and Pm (Z = 61). The database comprises a total of 8172 primary γ rays and 29605 secondary γ rays (a total of 37777 γ rays) associated with 12564 levels.

- [1] R.B. Firestone et al., "Database of Prompt Gamma Rays from Slow Thermal Neutron Capture for Elemental Analysis", IAEA STI/PUB/1263, 251 (2007).
- [2] Z. Revay, R.B. Firestone, T. Belgya, G.L. Molnar, "Handbook of Prompt Gamma Activation Analysis", edited by G.L. Molnar (Kluwer Academic Dordrecht, 2004), Chap. Prompt Gamma-Ray Spectrum Catalog, p. 173.

```
import pyEGAF as egaf
e = egaf.EGAF()
edata = e.load_egaf()
```

✓ 4.4s Python

Loading EGAF data sets, please wait...
All 245 JSON-formatted EGAF data sets loaded.

```
ensdf_C=e.get_ensdf(edata,"C13")
```

✓ 0.0s Python

```
13C 12C(N,G) E=THERMAL: {~EGAF}
13C c Evaluated Gamma-ray Activation File (EGAF).
13C 2c Evaluated by R.B. Firestone (LBNL), December 2003.
13C c BR${s{-0}}=0.00387 {I3} (2018MuZY)
13C cG RI$Elemental |s{|g} assuming %Abundance=98.93 8
13C N 1.0111 3 0.00387 3
13C PN
13C 2PN Thermal cross section in barns.
13C cN NR$Isotopic |s{|g}=NR*RI.
13C 2cN Divide by |s{-0} for intensity per neutron capture.
13C L 0.0 1/2- STABLE
13C L 3089.451 91/2+ 1.07 FS 10
13C G 3089.057 91.65E-05 8
13C L 3684.480 91/2- 1.10 FS 9
13C G 595.015 9 9.5E-06 4
13C G 3683.920 9 0.00122 3
```



Method	Equation	Notes
1	$\sigma_{th} = \frac{\sigma_{\gamma}}{\theta P_{\gamma}}$	P_g must be known, for example from beta decay if the nucleus captured a neutron is unstable.
2	$\sigma_{th} = \sum_{f=1}^{n-1} \sigma_{\gamma C \rightarrow f} (1 + \alpha_f)(1 + PCC_f)$	The sum of all primary transitions from the capture state can be used for nuclei with relatively simple decay scheme.
3	$\sigma_{th} = \sum_{i=2}^n \sigma_{\gamma i \rightarrow g.s.} (1 + \alpha_i)(1 + PCC_i)$	The sum of all ground state transitions can be used for nuclei with relatively simple decay scheme. Conversion coefficients must be known.
4	$\sigma_{th} = \sum_i E_i \sigma_{\gamma i} (1 + \alpha_i)(1 + PCC_i) / B_n$	The energy weighted sum can be used for any nuclei with resolved gamma-transitions. E_i is the energy of the transition, B_n is the binding energy and PCC is the pair conversion.

The electron conversion coefficients α_i are to be known

The pair conversion coefficients, PCCs, are usually rather small, and they have to be considered only for high-precision calculations

Budapest Neutron Centre Centre for Energy Research

Monte-Carlo calculations





Determination of quantities by computer simulation, using models of the physical processes and random numbers

Inputs:

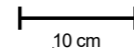
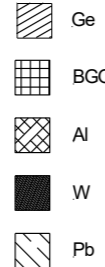
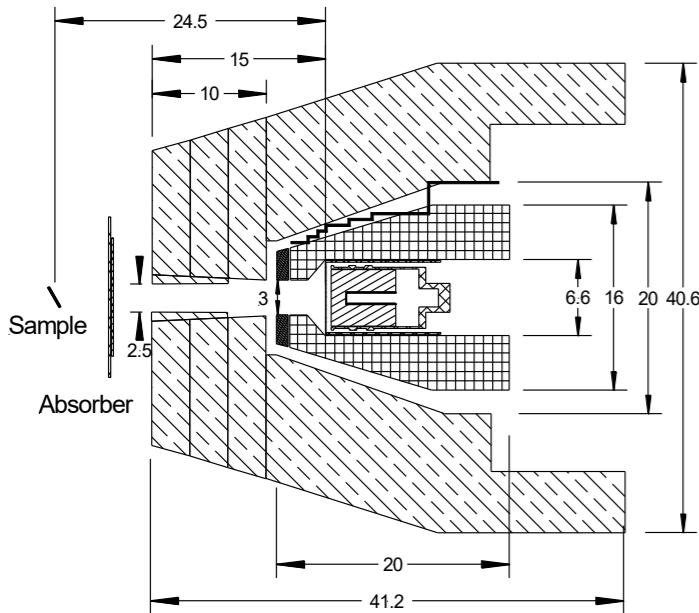
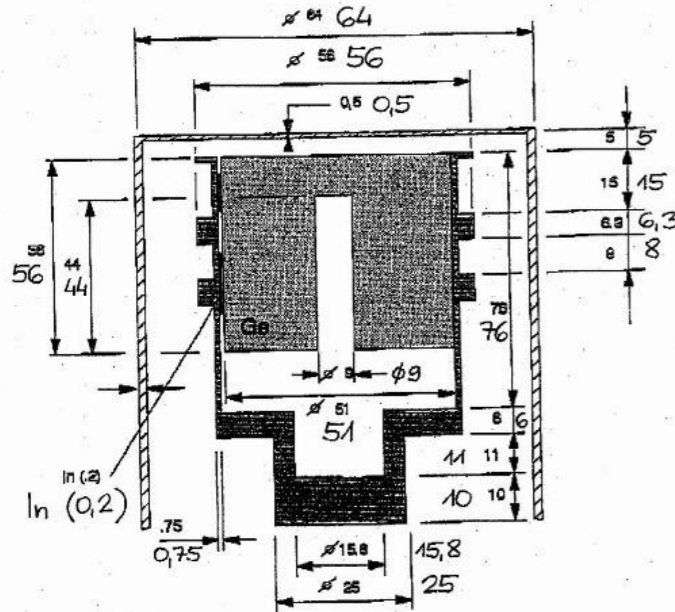
- Geometry of the HPGe detector, BGO Compton suppressor, sample chamber neutron and gamma shielding
 - Engineering drawings, optimization of unspecified dimensions, e.g. the dead layer thickness
 - Szentmiklósi, L.; Berlizov, A. N. Characterization of the Budapest Prompt-Gamma Spectrometer by Monte Carlo Simulations. Nucl. Instruments Methods A 2009, 612 (1), 122–126. DOI 10.1016/j.nima.2009.09.127.
 - Szentmiklósi, L.; Kis, Z.; Belgya, T.; Berlizov, A. N. On the Design and Installation of a Compton–Suppressed HPGe Spectrometer at the Budapest Neutron-Induced Prompt Gamma Spectroscopy (NIPS) Facility. J. Radioanal. Nucl. Chem. 2013, 298 (3), 1605–1611. DOI 10.1007/s10967-013-2555-2.
- Detailed geometry of the sample
 - Analytic definition, assembled from elementary planes, objects using inside/outside, union/intersection operations
 - Reproduction of the experimental arrangement, sample placement
- Neutron beam properties
 - T. Belgya, Z. Kis and L. Szentmiklósi, Neutron Flux Characterization of the Cold Beam PGAA-NIPS Facility at the Budapest Research Reactor, Nucl. Data Sheets, 2014, 119, 419–421, DOI: 10.1016/j.nds.2014.08.118
- Nuclear Data
 - Lib80x25: J. Lloyd Conlin, W. Haeck, D. Neudecker, D. Kent Parsons and M. C. White, LA-UR-18–24034: Release of ENDF/B-VIII.0-Based ACE Data Files, Los Alamos, 2018.

Outputs:

- Neutron beam intensity map
- Neutron capture rate map -> Conversion to gamma emission rates
- Gamma self absorption and neutron self shielding factors -> To correct the masses and concentrations



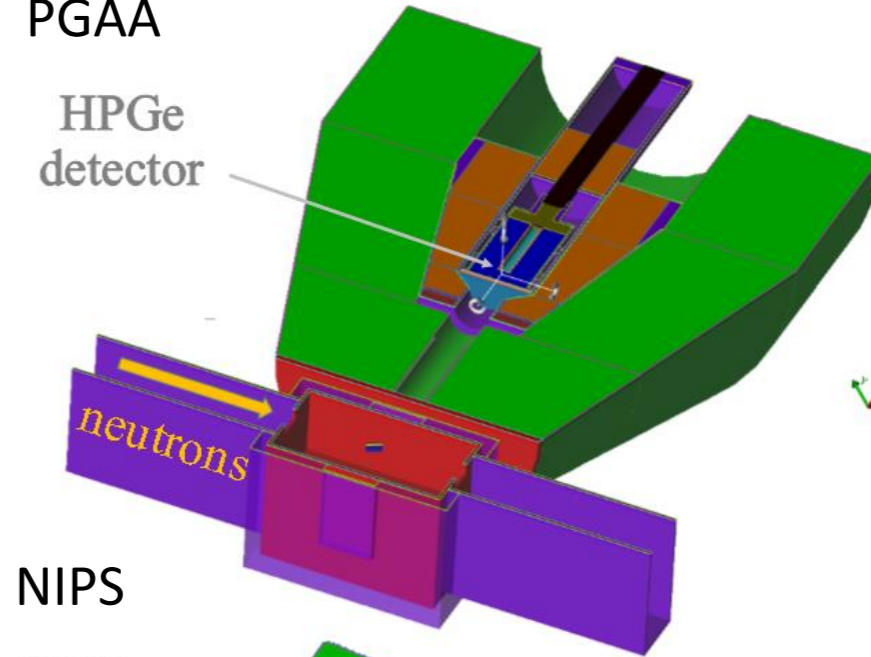
Engineering drawing -> MCNP input file -> sample -> simulation -> visualization of the results



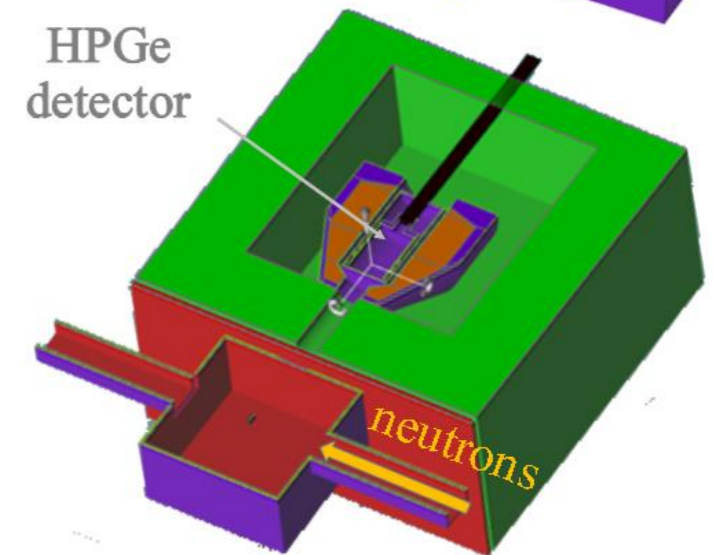
```

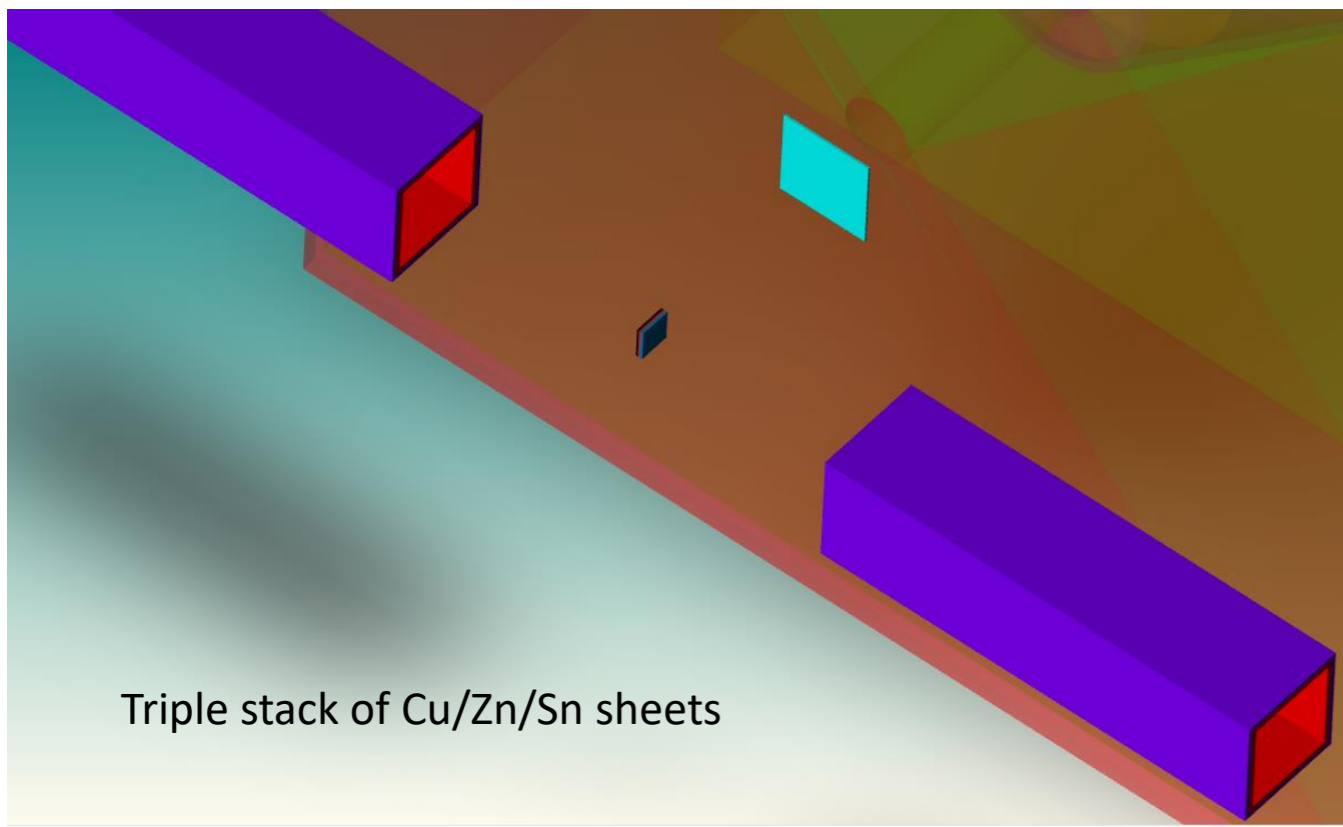
Lyster - [d:\MCNPWork\NORMA_metal_sandwich\Rot0\CuZnSn_00.inp]
-----
Fajl Szerkesztés Beállítások Kikódolás Súgó
c ISOCENTER in measurements = (0 -27.3 0)
c ISOCENTER in simulations = (0 -27.3 0)
c detector in measurements: Canberra GR2318/S HPGe + Scionix BGO
c detector in simulations: Canberra GR2318/S HPGe + Scionix BGO
c
c THIS INPUT FILE IS TO CALCULATE:
c the number of the activated XX or YY atoms in the sample irradiated in a
c position shifted and/or rotated around ISOC.
c We need only the number of gammas with specific energies reaching the
c entrance surface of the HPGe detector. Moreover, we need a ratio between
c the number of gammas in the different positions.
c
c
c
c **** TO ACTUALIZE THE SETUP ONE SHOULD CHANGE ONLY THE FOLLOWING CELLS ****
c **** FOR THE SAMPLE ITSELF: CELL NUMBERS STARTING WITH 5XX ****
c **** FOR THE AIR AROUND THE SAMPLE: CELL WITH NUMBER 900 ****
c
c
c ***** IRRADIATED OBJECTS SHOULD BE SET *****
c ***** USING SAMPLE POSITIONING *****
c
c ===== CELLS =====
c =====
c
c HPGe DETECTOR, always three characters beginning with "1"
100 1 -5.32 (-9 1 -3):(9 -2 10 -3) & $ Ge detector; 1 -5.32
    imp:n=1 imp:p=1 $
102 0 (7 -2 -8) ) imp:n=1 imp:p=1 $ empty core of detector
103 1 -5.32 (9 -7 -10):(9 -7 -10) & $ Ge dead layer around core
    (-10 8 7 -2) ) imp:n=1 imp:p=1
110 5 -2.702 15 -16 -17 imp:n=1 imp:p=1 $ front Al cap
111 5 -2.702 (16 -17 18 -5) imp:n=1 imp:p=1 $ side Al cap
114 0 16 -1 -18 #998 imp:n=1 imp:p=1 $ vacuum in Al (front)
998 0 -998 imp:n=1 imp:p=1 $ to tally photons through det entrance
115 0 (1 -27 -18 32)#(1 -36 32 -35):(1 -27 -18 32):(37 -38 32 -35)
    imp:n=1 imp:p=1
c
116 0 (27 -34 -18 31):(29 -34 33 -18) & $ vacuum in Al (outside back)
    (29 -34 33 -18) imp:n=1 imp:p=1
120 5 -2.702 (26 -27 30 -32):(27 -28 30 -31):(27 -28 30 -31) & $ Catcher holder
    (28 -29 -31 33) ) imp:n=1 imp:p=1
121 5 -2.702 (1 -26 3 -32) ) imp:n=1 imp:p=1 $ detector holder Al
122 0 (2 -26 -3) & $ vacuum in Al (inside back)
    (26 -28 -30) ) imp:n=1 imp:p=1
123 8 -8.933 (28 -99 -33) ) imp:n=1 imp:p=1 $ cold-finger
124 5 -2.702 (34 -5 -18 33) ) imp:n=1 imp:p=1 $ back Al cap
125 5 -2.702 (1 -36 32 -35) ) imp:n=1 imp:p=1 $ mounting bands
126 5 -2.702 (37 -38 32 -35) ) imp:n=1 imp:p=1
127 5 -2.702 (39 -40 32 -35) ) imp:n=1 imp:p=1
c
c BGO DETECTOR, always three characters beginning with "2"
213 6 -7.130 (44 -45 -42 41 -43 -52):(42 -45 52) & $ cylindrical part of BGO
    (-42 -45 52) imp:n=1 imp:p=1 $ LLD=0.12
219 6 -7.130 (-25 59 20 -43):(25 59 20 -43) & $ BGO
    (-15 25 54 -43) imp:n=1 imp:p=1 $ LLD=0.12
228 5 -2.702 (-43 -45 42 -47) ) imp:n=1 imp:p=1 $ BGO out cover triang
229 6 -7.130 (15 -44 41 -43) ) imp:n=1 imp:p=1 $ LLD=0.12 $ BGO front block
999 4 -7.130 (44 -45 42 -47) ) imp:n=1 imp:p=1 $ LLD=0.12 $ BGO back part
    
```

PGAA

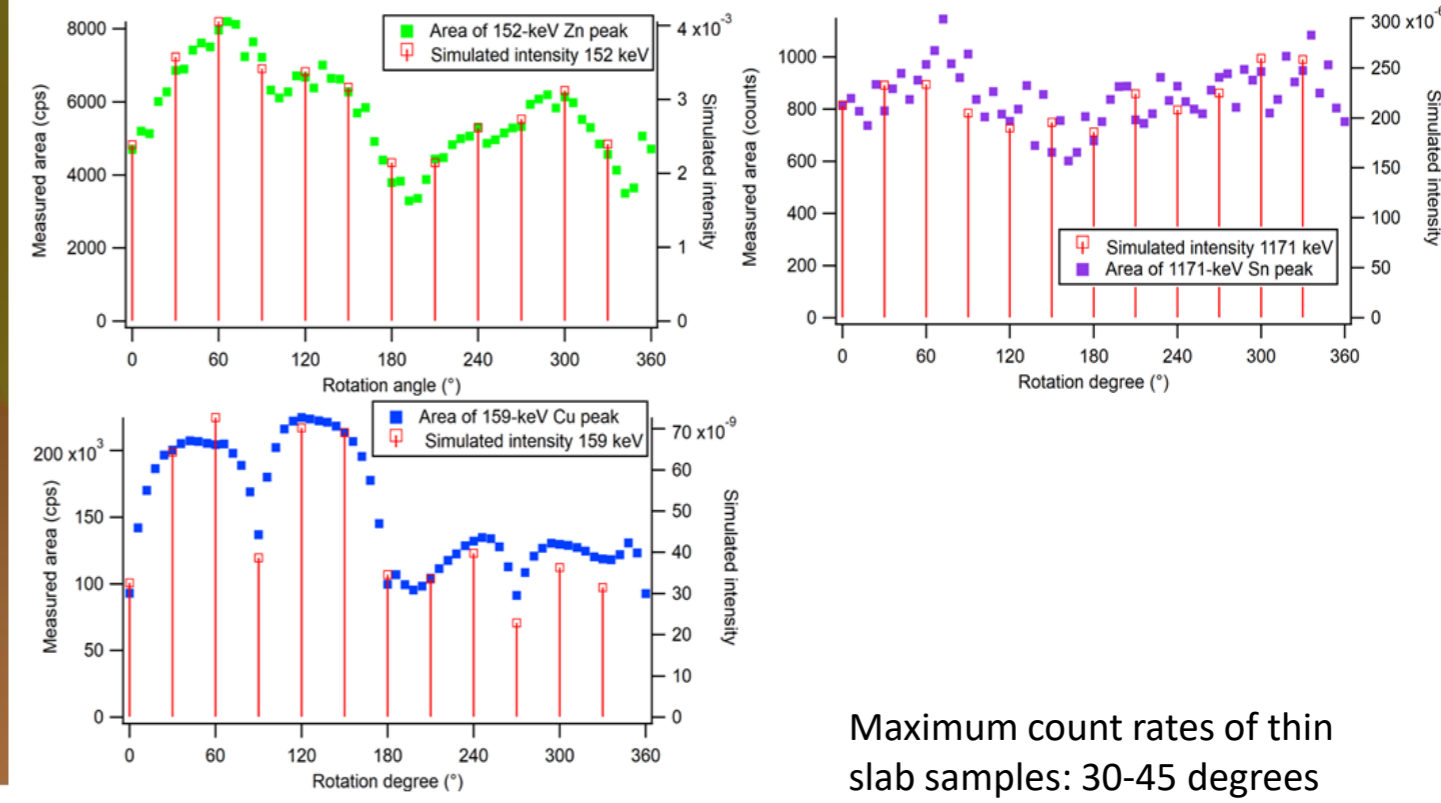


NIPS



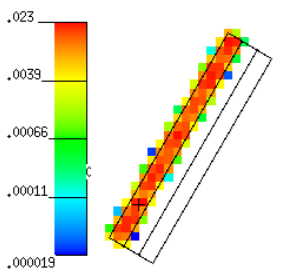


Experimental vs simulated prompt gamma count rates of elements at different angles

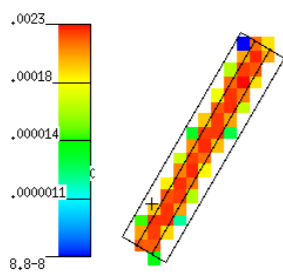


Maximum count rates of thin slab samples: 30-45 degrees rel. to the beam axis

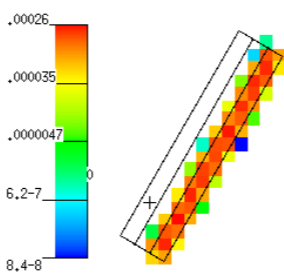
Cu neutron absorption (0.023)



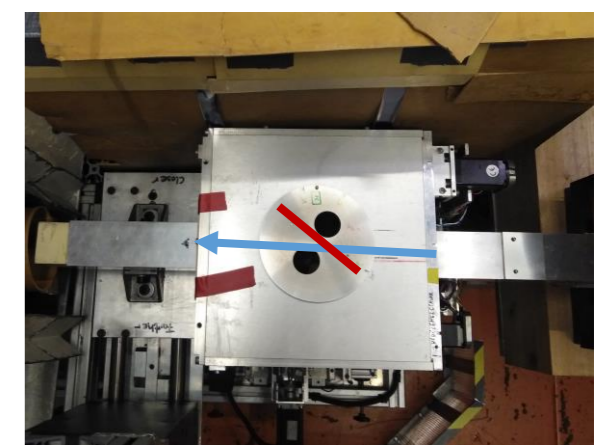
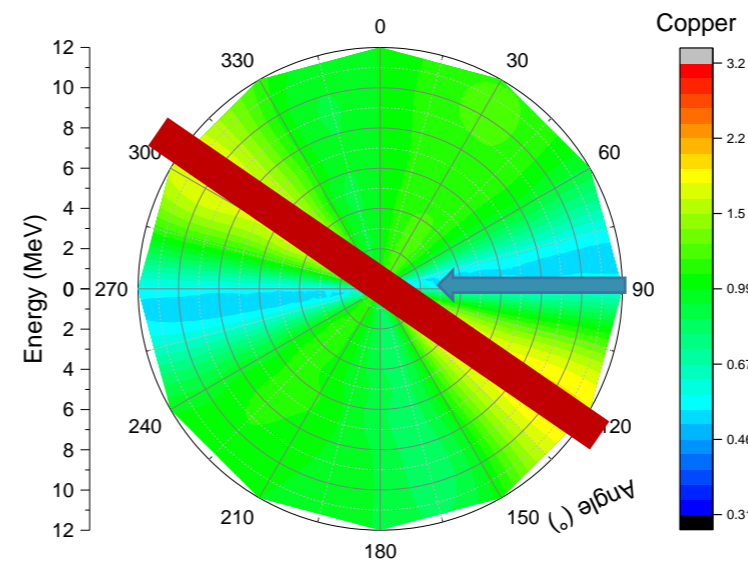
Zn neutron absorption (0.0023)



Sn neutron absorption (0.00026)



neutron beam





- Slow neutron beams are useful to determine thermal neutron capture cross-sections
- Can be used as an anchor value for energy-dependent cross-section measurements by ToF method
- Accurate gamma detector calibration is required to provide high-quality results
- The measurement equations and related uncertainty budgets are transparent
- BNC has 20+ years of experience in this area, the experimental facilities and our competences are openly available via Transnational Access Programs

Thank you for your attention!

